

Original Article

Mechano-Physical Properties and Microstructure of Colloidal Nanosilica-Incorporated Volcanic Ash-Based Geopolymer Mortar after Exposure to Elevated Temperatures

Samson Kiprop¹, Richard Ocharo Onchiri², Naftary Gathimba³

¹Department of Civil Engineering, Pan African University Institute of Basic Sciences, Technology and Innovation, Nairobi, Kenya.

²Department of Building and Civil Engineering, Technical University of Mombasa, Mombasa, Kenya.

³Department of Civil, Construction and Environmental Engineering, Jomo Kenyatta University of Agriculture and Technology, Nairobi, Kenya.

¹Corresponding Author : kiprop.samson77@gmail.com

Received: 02 January 2024

Revised: 05 April 2024

Accepted: 04 May 2024

Published: 26 May 2024

Abstract - Due to the expansion of construction activities and the increased threat of fires to civil structures and lives, there has been a need to find alternative fire-resistant materials that meet sustainability and green material standards. This study reports on using Colloidal Nanosilica (CNS) to modify the elevated temperature resistance of Volcanic Ash-Based Geopolymer Mortar (VAGPM). The volcanic ash (VA) locally sourced in Kenya was partially replaced with between 1-5% CNS by mass of VA and activated with sodium or potassium hydroxide and sodium silicate. The workability of the resulting mixtures was determined. Following a curing period of 28 days, the VAGPM specimens were exposed to temperatures ranging from 200-800°C for durations of 1 and 2 hours, and their compressive strengths, mass losses, volumetric changes, visual appearances, and microstructural properties were analysed. Results indicated that replacing VA with CNS up to 5% by mass resulted in a reduction in the flowability of the fresh mortar and that adding 2% CNS improved compressive strength and elevated temperature resistance. In contrast, higher levels did not significantly improve performance. Specimens recorded increased compressive strengths up to 400 and 600°C. Increasing CNS levels decreased mass loss and volume shrinkage. The samples also displayed changes in colour and mineralogical phases after exposure to elevated temperatures. CNS yielded a denser microstructure.

Keywords - Colloidal Nanosilica, Elevated temperature, Geopolymer mortar, Mechano-physical properties, Volcanic ash.

1. Introduction

Fire is among the disasters that pose a serious hazard to both life and civil structures in both urban and rural settings, although fire is critical to human society's evolution [1-4]. Each year, fire claims thousands of lives and destroys properties worth billions of dollars [1]. The extent of damage experienced by a building in a fire incident is influenced by both the rise in temperature and the duration of exposure to the fire [5]. The ability to withstand elevated temperatures brought on by fires is one of the fundamental safety requirements when designing construction projects, including high-rise buildings and tunnels. In these circumstances, materials could be subjected to elevated temperatures to assess their resistance [6]. Construction activities have expanded rapidly worldwide in response to increased infrastructural demand in the past two decades. Cement stands out as one of the most widely used materials in construction activities.

Globally, it is estimated that approximately 2.8 billion tons of cement are manufactured yearly, and it is anticipated to increase to 4 billion tons annually by 2050 [7]. Cement manufacturing uses much energy since its production temperatures need to be raised to a range of 1350°C-1450°C, and this results in an increase in consumption of the limited natural mineral coal resources. Additionally, cement manufacture produces carbon dioxide, which contributes to global warming [8-12]. Research studies have reported that subjecting conventional cement concrete to high temperatures can result in damages, including colour changes in concrete as well as have a significant impact on its modulus of elasticity, compressive strength, and density, commencing at 105°C. Concrete can also lose up to 50% of its original strength when subjected to temperatures within the range of 400°C to 500°C due to the dehydration of calcium hydroxide [6,13-15]. The heated layers tend to separate and disintegrate from the cooler



inner layers as they reach higher temperatures [16]. The construction sector faces growing demands to explore alternative cementing materials that meet sustainability and green material standards [17–20]. Furthermore, the risk of fires has prompted a search for innovative fire-resistant materials to ensure structures are stable in the face of substantial fire incidents. In this context, geopolymers that utilise alumino-silicate-rich industrial wastes like fly ash or naturally occurring materials like natural pozzolans in combination with alkaline activators stand out as an environmentally friendly substitute to the conventional cement binder [21–23]. Geopolymers achieve structural capacity through the polycondensation process of silicon oxide and aluminium oxide. Therefore, geopolymers do not depend on the creation of calcium silicate hydrate gel for the development of their matrix and strength [24]. Geopolymers have recently gained increasing attention from scientists and engineers due to their environmentally friendly and sustainable qualities, which can help reduce greenhouse gas emissions [25]. Geopolymer binders produce significantly lower CO₂, amounting to up to nine times less, and demand six times less operational energy consumption when compared with Portland cement [26]. A Geopolymer is an amorphous compound characterized by optimal attributes akin to rock-forming elements, encompassing features like hardness, chemical stability, and durability [27]. Compared to conventional concrete, geopolymers have excellent thermal stability because of their inorganic structure [28]. At elevated temperatures, geopolymers display a remarkably low thermal conductivity and do not release harmful gases when exposed to heat [16]. Despite these advantages, there is limited research on the behaviour of geopolymer cement and mortar in the context of fire exposure to their surface [6].

Nanoparticles have recently been introduced into building materials to enhance their durability and physical and mechanical properties and improve their performances [29]. The word “Nanomaterials” typically refers to ultrafine powder that is less than 100 nm and can contain organic and inorganic materials [3,30]. Nanoparticles like nanosilica and nano-alumina are crucial for enhancing the characteristics of geopolymers. They offer extra active nucleation sites, boost the pozzolanic reaction, and create a nano-filling effect, resulting in densification of the geopolymer microstructure system. This leads to significant improvement in the Interfacial Transition Zone (ITZ) and pore structure. This helps arrest cracks and provides better interlocking bonds between slip planes in the geopolymer matrix [16,31,32].

Several studies have demonstrated the effectiveness and use of nanosilica in cementitious composites exposed to high temperatures [33,34]. Nanosilica typically enhances compressive strength across various temperature ranges [35] and leads to higher residual compressive and tensile strengths while mitigating specimen mass loss and spalling [34]. Rashad and Ouda [3] employed nanosilica to enhance fire resistance

of geopolymer pastes derived from metakaolin and reported that incorporating 0.5% of nanosilica resulted in a notable improvement of up to 9% and 10% in the compressive strength of the geopolymer specimens at 7 and 28 days, respectively. Moreover, the residual compressive strength following exposure to high temperatures demonstrated an average increase of 8.19% in contrast to the control geopolymer specimen without nanosilica, indicating enhanced resistance to increased temperatures. In another study examining the impact of nanosilica on the compressive strength of geopolymer derived from fly ash precursor material and subjected to elevated temperatures, Shaikh and Haque [36] observed that the inclusion of nanosilica improved the residual compressive strength, with the geopolymers having 2% nanosilica exhibiting the lowest reduction in mass and volume. Ibrahim et al. [1] noted a significant reduction in pore size distribution for material specimens containing colloidal nanosilica, suggesting the formation of denser specimens. In the study by Deb et al. [37], the 90-day mass loss of geopolymer, when immersed in an acid solution, decreased from 6% to 1.9% with the addition of 2% nanosilica, implying an enhancement in durability.

Studies have reported that several factors influence the properties of geopolymers, including the mineralogical and chemical makeup of the starting materials, the particle sizes, the nature of the alkaline solution used, the curing conditions, the liquid-to-solid ratio, and temperatures [38,39]. The extent to which each aspect affects the performance of geopolymer materials and their interaction are gradually being examined with the increase in experimental studies [39]. The scientometric review by Paul et al. [40] identified some of the critical research areas for geopolymers, including the type of geopolymers, the Geopolymer mechanical and durability properties, microstructure, and their applications.

The use of an alkaline activator is essential to dissolve Al and Si in the precursor, resulting in geopolymer formation. The careful selection of the activator is crucial since the activator composition results in a varying effect on the properties of both freshly prepared and solidified geopolymers [22], as well as their thermal properties [28]. Commonly used alkaline activator solutions include sodium hydroxide (NaOH), sodium silicate (Na₂SiO₃), potassium hydroxide (KOH), and potassium silicate (K₂SiO₃) [41]. The alkaline solutions supply the alkali-metal cations, raise the mixture’s pH, and accelerate the source material dissolution, which promotes geopolymer strength development [42]. At high temperatures, Hosan et al. [23] noted that fly ash geopolymers activated with potassium-based solutions exhibited greater thermal stability than those made with sodium-based activators, showing superior remaining compressive strengths, less reduction in mass, decreased volumetric reduction, and fewer cracks. Some studies found that the best activator is a sodium silicate solution mixed with potassium hydroxide [43,44].

The silicate solution enhances the dissolution process by providing Si ions in the aqueous phase, which helps in activating the geopolymer material precursor [45]. The silicate solution also leads to higher reaction rates, resulting in better strength and microstructure properties [22,46]. Furthermore, the silicate of the resulting solution provides additional silicon dioxide and hydroxide, ensuring that the solution has a high alkalinity level [47]. Different alkali activators significantly impact compressive strength even with no addition of a silicate solution [45]. According to the fire resistance study by Alouani et al. [7], geopolymer binders produced by KOH with Na_2SiO_3 were stable up to 600°C.

However, at 800°C, small cracks were observed, increasing with a higher percentage of NaOH in the geopolymers. In contrast to sodium ions, potassium ions accelerate the condensation rate to a greater extent, leading to a more efficient polycondensation process which leads to the creation of a more compact and heat-resistant geopolymer. Additionally, the compressive strengths are significantly impacted by the alkaline activator concentration [48]. Several studies have also indicated that geopolymers manufactured from NaOH exhibit a higher compressive strength at ambient temperature than KOH-activated geopolymers, regardless of the curing condition [45].

Several raw materials, such as fly ash [49,50], metakaolin [51], volcanic tuff [16], volcanic ash [52], and blast furnace slag [53], containing silica and alumina bearing phases have been used as precursors in geopolymers. While various source materials can be employed in geopolymer production, the geopolymers produced with fly ash have garnered the most attention [54]. Despite the exciting applications and the ease with which volcanic ashes can be obtained from numerous untapped deposits worldwide, there has been limited research on their utilization [55].

Volcanic ash is a term that specifically denotes the fine fragments of pyroclastic materials, each measuring less than 2mm in size [56]. Volcanic ash deposits are approximately 0.84% (124 million Ha) of the world's land cover, with about 60% of this in tropical countries [42,57]. While volcanic ash has been utilised as a geopolymer precursor material [58], the resulting specimen has shown slightly lower reactivity and slower strength development. It may exhibit swelling and some cracks compared to geopolymers resulting from alternative precursor materials such as fly ash [59].

While previous research studies have reported that nanosilica can enhance the properties of cementitious composites exposed to elevated temperatures, understanding the performance of volcanic ash-based geopolymers containing Colloidal Nanosilica (CNS) under elevated temperatures remains limited. The current study aims to address this gap by evaluating the performance of volcanic ash-based geopolymer mortar containing CNS in both pre-and

post-exposure to elevated temperatures. Two different alkaline activators were employed: sodium hydroxide with sodium silicate ($\text{NaOH-Na}_2\text{SiO}_3$) and potassium hydroxide with sodium silicate ($\text{KOH-Na}_2\text{SiO}_3$). Geopolymer specimens underwent exposure to both ambient and elevated temperatures (200°C, 400°C, 600°C, and 800°C) for durations of 1 and 2 hours.

This study assessed the impact of various CNS levels, ranging from 0 to 5% by weight, as a partial substitute of volcanic ash in both activation methods of geopolymers. Workability was examined for mixtures with different CNS levels.

The investigation encompassed evaluations of compressive strengths, mass losses, volume changes, and alterations in the visual appearance of geopolymers to understand their response to elevated temperatures. Observations of the geopolymer's microstructure using X-ray Diffraction (XRD) and Scanning Electron Microscopy (SEM) provided additional insights into the mechanical and physical behaviour, as well as the various mineral phases present in the geopolymer.

The current research findings contribute to the understanding of how CNS affects volcanic ash-based geopolymer behaviour pre- and post-exposure to elevated temperatures. The insights from the current study will be a valuable reference for future research on employing volcanic ash geopolymers with CNS in high-temperature engineering constructions.

2. Materials and Methods

2.1. Materials

2.1.1. Volcanic Ash

The volcanic ash used in this research was sourced from the Simba area in Kajiado County of Kenya, geographically located at 2°10' 27.2" S and 37° 38' 35.2" E with an elevation of 1000m above sea level. After collection, the ash was dried at 105°C for 24 hours and subsequently ground to achieve a particle size finer than 45µm. X-ray fluorescence spectrometry (XRF) was employed to analyse the chemical composition of the volcanic ash, and the results are presented in Table 1.

Table 1. Chemical composition of (wt%) volcanic ash

Chemical	Composition (%)
Silica (SiO_2)	47.91
Alumina (Al_2O_3)	14.91
Iron Oxide (Fe_2O_3)	9.39
Lime (CaO)	12.31
Magnesium Oxide (MgO)	10.79
Sodium Oxide (Na_2O)	3.60
Potassium Oxide (K_2O)	1.47
Phosphorus Oxide (P_2O_5)	0.73

The chemical makeup of the ash revealed that SiO₂, Al₂O₃, CaO, MgO, and Fe₂O₃ were the principal oxides. Notably, SiO₂, Al₂O₃, and Fe₂O₃ collectively accounted for 72.21%, surpassing the ASTM standards' minimum requirement of 70% [60]. The Kenyan volcanic ash used was classified as basaltic since its SiO₂ content was less than 52.5% by weight [56]. The X-ray Diffraction (XRD) analysis patterns, illustrated in Figure 1, and the Scanning Electron Microscope (SEM) micrograph, shown in Figure 2, offered insights into the characteristics of the Kenyan volcanic ash. The XRD diffractograms indicated a combination of amorphous and crystalline phases, including augite, maghemite, forsterite, hematite, albite, diopside, alkali feldspar, and wollastonite. Certain minerals, such as augite, suggested that the ash could have good reactivity with the alkaline solutions [56,61]. The specific gravity of the ash was found to be 2.78. The SEM image in Figure 2 illustrates the irregular morphology of the volcanic ash, displaying varying shapes and sizes.

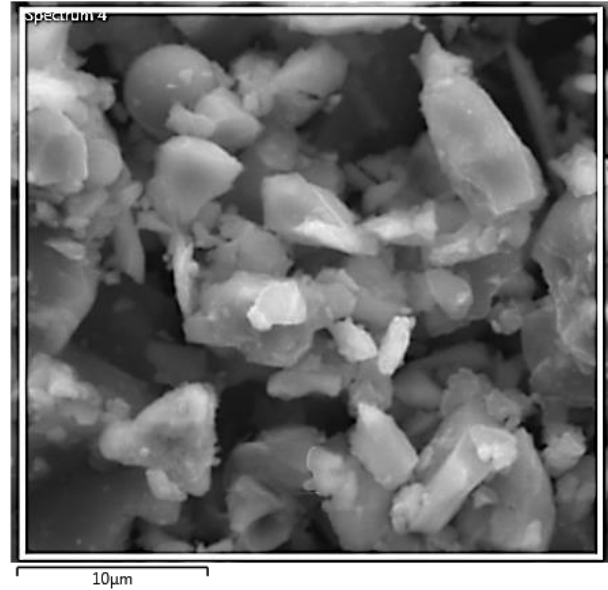


Fig. 2 SEM image of the VA

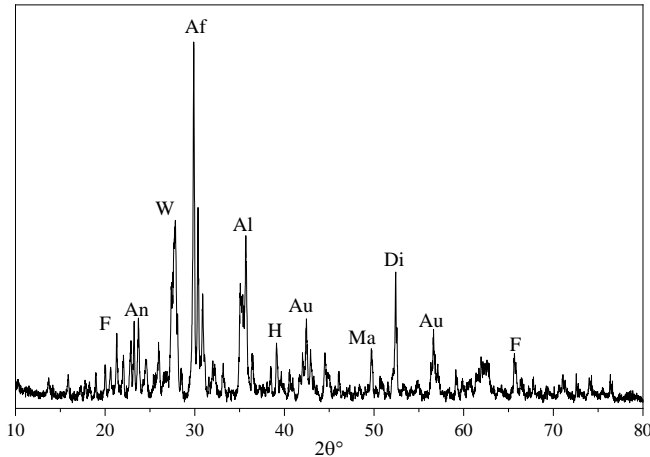


Fig. 1 XRD patterns of VA

[Note: Au: Augite, Al: Albite, Ma: Maghemite, Di: Diopside, Af: Alkali-Feldspar, H: Hematite, F: Forsterite, W: Wollastonite, An: Anorthite]

2.1.2. Alkaline Activator Solutions

The alkali activators employed in the geopolymer production comprised sodium hydroxide (NaOH) solution and sodium silicate (Na₂SiO₃) solution, as well as potassium hydroxide (KOH) and sodium silicate (Na₂SiO₃) solution. The NaOH and KOH solutions were produced by dissolving analytical-grade NaOH or KOH pellets in distilled water to make a 10M solution. These 10M NaOH and KOH solutions were prepared and stored at ambient temperature for a minimum of 24 hours before being used. The ratio of liquid Na₂SiO₃ to NaOH or KOH solution used was 2.5. The properties of the alkaline activators from the manufacturer are outlined in Table 2. Figure 3 displays the images of the VA, CNS, NaOH, Na₂SiO₃, and KOH samples utilised in the experimental studies involving volcanic ash with colloidal nanosilica.

Table 2. Alkaline activators properties

Properties	Sodium Hydroxide	Potassium Hydroxide	Sodium Silicate
Molar mass, (g/mol)	39.997	56.11	122.06
Silica (SiO ₂) (%)	-	-	29.55
Sodium Oxide (Na ₂ O) (%)	-	-	14.07
Water (H ₂ O)	-	-	56.38
Specific gravity	2.13	2.04	1.53
Colour	White	White	Greenish to colourless

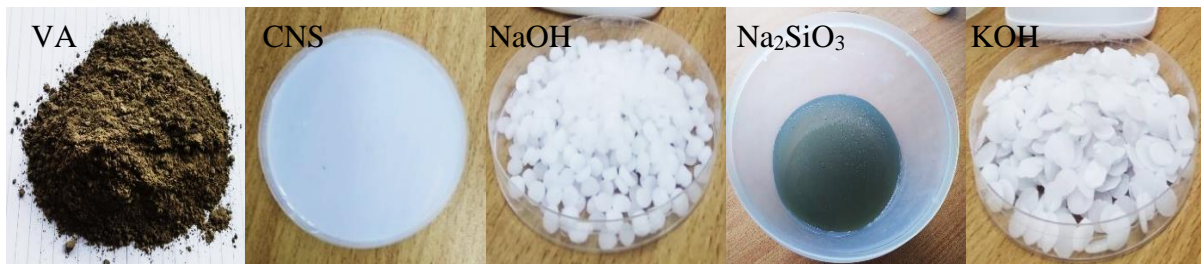


Fig. 3 The geopolymer raw materials used in the experimental studies

Table 3. Colloidal nanosilica (Chemical and physical) properties

Nanosilica	
Properties	Value
Nanosilica (%)	50.23
Water (%)	49.77
Specific gravity	1.395
pH value (at 25 ⁰ C)	9.51
Viscosity (sec)	10.79
Specific surface area, SSA (in m ² /gm)	85
Average particle size (in nm)	35.29
Colour	Transparent to cloudy white
Loss on Ignition	≤1

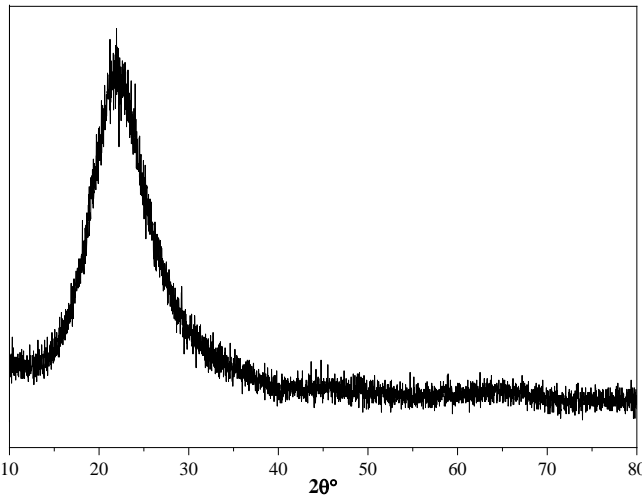


Fig. 4 The XRD plot of CNS

2.1.3. Colloidal Nanosilica (CNS)

Water-dispersed CNS was obtained from Bee-chems Chemicals Ltd., Kanpur, Uttar Pradesh, India. Table 3 gives the properties of the CNS. The nanoparticles had an average diameter of 35.29 nm. CNS has been reported to have superior dispersibility of silica nanoparticles compared to powdered nanosilica. Additionally, it exhibits better initial strength improvement attributed to a rapid initial hydration reaction [62]. Regarding the strength properties of mortar, CNS is more effective than agglomerated silica [63]. Figure 4 illustrates the XRD plot of the colloidal nanosilica. The observed broad peak detected at about 22° of the 2θ scale indicates the amorphous character of the silica.

2.1.4. Fine Aggregates

The fine aggregates utilized consisted of natural river sand and had a specific gravity of 2.51 and a water absorption rate of 2.81%, as measured in the laboratory to ASTM standards [64]. The fineness modulus was 2.53. Figure 5 depicts the fine aggregate grading. The fine aggregates were classified as well-graded, meeting the particle size distribution criteria outlined in the standards [65].

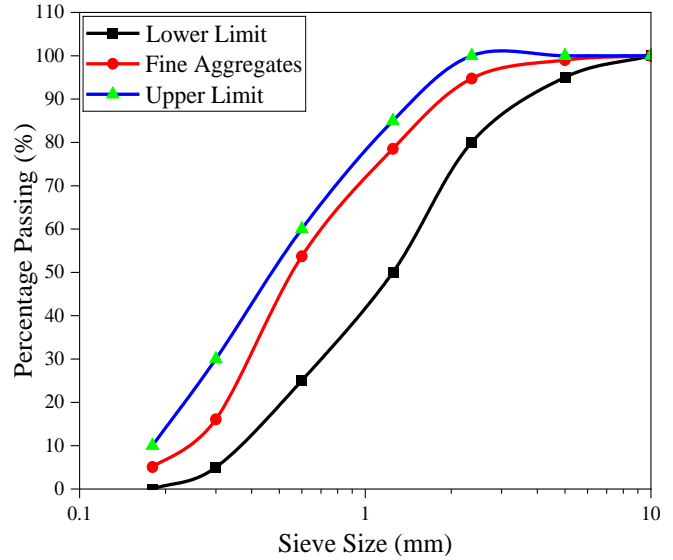


Fig. 5 Fine aggregates particle size grading

2.2. Methods

2.2.1. Mix Proportions

A total of twelve geopolymers mortar mixes were prepared. The first mix for each activation method was used as the reference having volcanic ash without any content of CNS. The reference mixtures were marked as NS0 and KS0 for NaOH-Na₂SiO₃ and KOH-Na₂SiO₃ activation methods, respectively. The other five mixtures for each activation method were prepared by partially substituting volcanic ash with CNS at 1%, 2%, 3%, 4%, and 5% by mass of VA. The mixes for NaOH-Na₂SiO₃ activation were marked as NS1, NS2, NS3, NS4 and NS5, respectively, while the mixes for KOH-Na₂SiO₃ activation were marked as KS1, KS2, KS3, KS4 and KS5, respectively. A consistent alkaline solution-to-binder ratio (a/b) of 0.55 was maintained across all mixes. The 49.77% water content in the CNS (See Table 3) was considered in the total mixing water calculation to ensure a constant water-to-binder ratio was maintained. The ratio of the ash (with and without CNS) to sand was adopted as 1:2 [66]. Table 4 outlines the geopolymer mix proportions per cubic meter of geopolymer mortar.

2.2.2. Mixing, Casting, and Curing Procedures

The initial step involved mixing the dry volcanic ash with the fine aggregates in the mortar mixer for approximately 3 minutes. Subsequently, NaOH or KOH solution, along with the free water was gradually added to the dry mix, then followed by the addition of Na₂SiO₃. The mixing process continued for an additional 2 minutes before introducing CNS, at which point the mixing speed was increased and sustained for an additional 5 minutes. Following the mixing process, the flow of the mortar was assessed.

Fresh geopolymer mortars were then cast into 50x50x50 mm steel moulds and vibrated for 30 seconds to eliminate trapped air within the specimens.

Table 4. Mixes proportions

Mix	NS %	VA (kg/m ³)	CNS (kg/m ³)	NaOH (kg/m ³)	KOH (kg/m ³)	Na ₂ SiO ₃ (kg/m ³)	FA (kg/m ³)	Water (kg/m ³)
NS0	0	631.22	0	99.19	0	247.97	1262.43	35.48
NS1	1	624.91	12.57	99.19	0	247.97	1262.43	29.22
NS2	2	618.60	25.13	99.19	0	247.97	1262.43	22.97
NS3	3	612.28	37.70	99.19	0	247.97	1262.43	16.72
NS4	4	605.97	50.27	99.19	0	247.97	1262.43	10.46
NS5	5	599.66	62.83	99.19	0	247.97	1262.43	4.21
KS0	0	631.22	0	0	99.19	247.97	1262.43	35.48
KS1	1	624.91	12.57	0	99.19	247.97	1262.43	29.22
KS2	2	618.60	25.13	0	99.19	247.97	1262.43	22.97
KS3	3	612.28	37.70	0	99.19	247.97	1262.43	16.72
KS4	4	605.97	50.27	0	99.19	247.97	1262.43	10.46
KS5	5	599.66	62.83	0	99.19	247.97	1262.43	4.21

*VA=Volcanic ash, NS=Nanosilica, FA=Fine aggregates. The total weight of the colloidal nanosilica was calculated as $CNS = (VA \times CNS\%) / 0.5023$.

Vinyl sheets were used to cover the moulds containing freshly mixed geopolymer mortar to prevent any moisture loss, thus ensuring the availability of a water media to facilitate the exchange of the Si and Al ions in the specimens [67,68]. The specimens were allowed to rest for 1 hour before being put in an oven at 105°C for 48 hours during the initial heat curing process. Afterwards, the geopolymer specimens were demoulded, covered with plastic bags, and underwent additional at ambient temperature. Tests were conducted at 28 days.

2.2.3. Experimental Tests

The flow of the mortar mixes was evaluated through the flow table method [69]. After 28 days, three cube specimens from each of the 12 mixes were exposed to varied levels of elevated temperatures, specifically 200, 400, 600, or 800°C. The heat was incrementally applied at a rate of approximately 5°C per minute from ambient temperature in an electric furnace (as illustrated in Figure 6) designed to reach a maximum temperature level of 3000°C. Once a target temperature (say 200, 400, 600 or 800°C) was reached, it was maintained for either 1 or 2 hours, depending on the sample heating regime. Subsequently, the electric furnace was switched off, allowing the mortar specimens to cool down to room temperature within the electric furnace. Considering previous studies reported that significant changes in the strength and the microstructure characteristics of geopolymers occur within the initial two hours [70], the geopolymer specimens were exposed to different levels of elevated temperatures for either 1 or 2 hours. Exposure duration of more than 2hrs has little effect on geopolymers [71]. Figure 7 illustrates the heating and cooling regimen of the specimens within the furnace. Additionally, a set of geopolymer samples from each of the 12 mixes was also left unexposed to elevated temperatures for comparative study. Finally, the compressive strengths of the test specimens were measured in triplicate, both pre and post-exposure to elevated temperatures following ASTM-C109 standards [72]. For each CNS level, exposure

temperature level, and duration, the compressive strength of each of the three specimens was tested, and the average of the test results was reported. Mass loss, volume shrinkage, visual appearances, and microstructure were also determined on the geopolymer specimens.

Mass changes of the geopolymer specimens were determined by measuring the masses pre- and post-exposure to high temperatures prior to the compressive strength tests. Volume changes were computed using calliper measurements taken pre- and post-exposure to elevated temperatures. Microstructure analysis involved grinding fragments from the tests, passing them through a 75µm sieve, and conducting XRD to detect geopolymer chemical and phase changes. Additionally, selected fragments from the tests underwent a Scanning Electron Microscope (SEM) investigation.

3. Results and Discussions

3.1. Workability

Figure 8 illustrates the flow characteristics of the geopolymer samples with and without CNS for NaOH-Na₂SiO₃ and KOH-Na₂SiO₃ mortar. The results revealed that for both activation methods, the mortar having CNS exhibited lower workability than the control mortar. As the level of CNS replacement increased, the mortar's flow value also decreased. The mixtures NS0 and KS0 displayed 106mm and 115mm flow values, respectively. Increasing the CNS level to 5% showed a reduction in flow by 17.9% for NaOH-Na₂SiO₃ mortar and 22.6% for KOH-Na₂SiO₃ mortar. The findings in workability showed consistency with the findings of previous research studies [62,73,74]. The reduction in flow could be ascribed to the high specific surface area of the nanosilica particles in comparison to the ash particles [37] and the water absorption potential of the silica nanoparticles [75,76], which in turn increases water demand. Moreover, owing to the high reactivity of nanosilica particles, there was a likelihood of water retention around them, contributing to the decrease in workability [3].

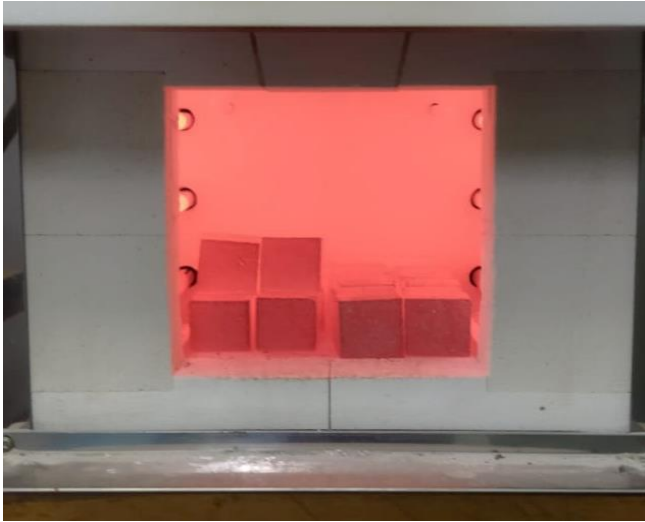


Fig. 6 Electric furnace with the mortar cubes

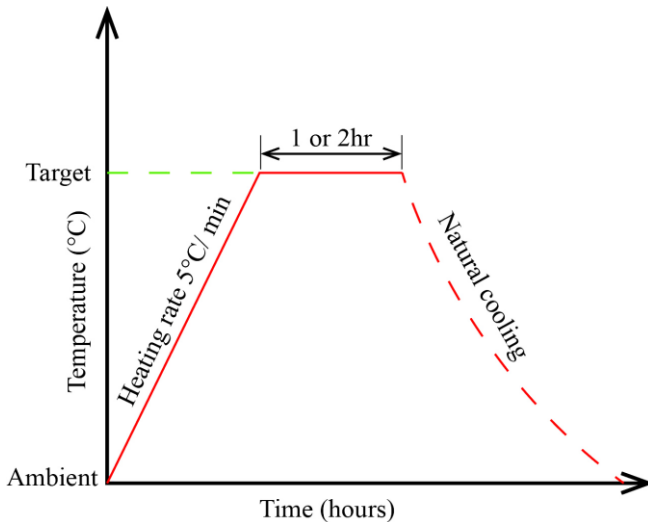


Fig. 7 Mortar cubes heating and cooling regime

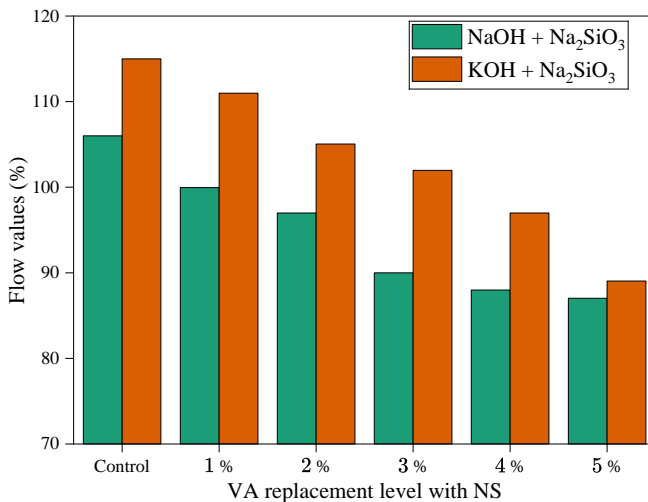


Fig. 8 The impact of CNS on the workability of the VA geopolymer mortar

The flow values for KOH-Na₂SiO₃-activated mortars were higher in comparison to the flow measurements of NaOH-Na₂SiO₃-activated mortars. The flow for KS0 was 8.5% higher than the flow for NS0. Notwithstanding, the 10M NaOH solution contains more water when compared with 10M KOH due to the difference in the molar masses. The reduced flow of mortar containing NaOH is linked to NaOH having a smaller Na⁺ cation, which may attract the components of both the mortar and the binder [77]. A pattern similar to the one recorded in the current study has been reported in other previous studies [75,78].

3.2. Initial Compressive Strength

The 28-day compressive strength results of the NaOH-Na₂SiO₃ and KOH-Na₂SiO₃-activated VA geopolymer mortars with the various CNS replacement levels are illustrated in Figure 9. The incorporation of CNS in the VA geopolymer displayed significantly elevated 28-day compressive strengths in comparison to the control mix from both activation methods. At the optimal CNS replacement level, the compressive strength showed enhancements of up to 18.4% for NaOH-Na₂SiO₃ activated geopolymer and up to 21.13% for KOH-Na₂SiO₃ activated geopolymer. The obtained results showed that 2% of CNS addition as a percentage of the weight of the VA precursor, is the optimum replacement level.

The CNS improved the compressive strengths of the geopolymer specimens by providing additional active nucleation sites. This resulted in enhancement of the pozzolanic activity and the nano-filling effect leading to geopolymer microstructure system densification. Furthermore, the pore structure and the ITZ of the aggregates and binder may have been greatly enhanced, which helped in arresting cracks and providing better interlocking bonds between slip planes in the geopolymer matrix [16,31,32], and this led to the increase in the compressive strength.

Beyond a 2% replacement level of CNS, a marginal improvement in compressive strength was observed for both geopolymers. KS5 recorded a compressive strength that was 5.4% higher than that of KS0, and NS5 exhibited a compressive strength nearly equal to that of NS0. The measured compressive strengths were reduced by 8.1%, 5.15%, 1.84% and 1.1% for NaOH-Na₂SiO₃ and 3.17%, 12.2%, 9.05% and 5.4% for KOH-Na₂SiO₃ geopolymer when the level of CNS replacement was increased to 1, 3, 4 and 5% respectively for both geopolymers. The insignificant strength increase with the increase in NS level past the 2% optimum level indicates that the excess silica discharged did not participate in further gel formation reactions [75]. Moreover, the use of higher amounts of CNS reduced the compressive strength. This behaviour could be linked to agglomeration resulting from the high surface area associated with silica nanoparticles [10] and possibly the creation of weak zones in the form of voids in the mortar samples [79,80].

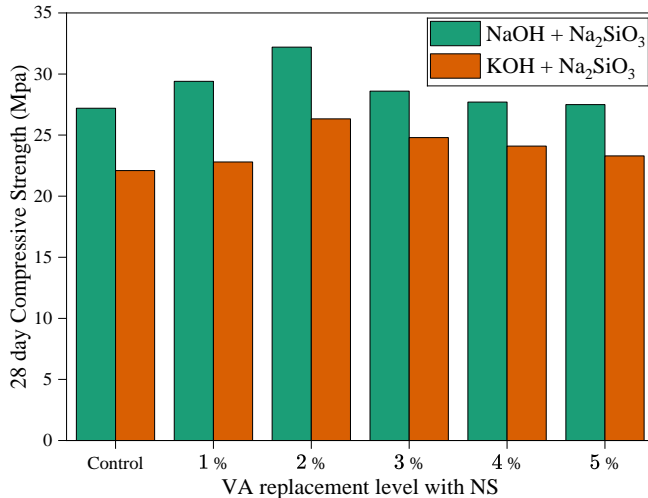


Fig. 9 Effect of nanosilica on the 28-day compressive strength of NaOH-Na₂SiO₃ and KOH-Na₂SiO₃ activated VA-based geopolymer mortar

It was also observed that 10M KOH-Na₂SiO₃ geopolymers had significantly lower compressive strength than 10M NaOH-Na₂SiO₃ counterparts across all geopolymers. The NaOH-Na₂SiO₃-activated geopolymer demonstrated the highest compressive strength, reaching 32.2 MPa, whereas the KOH-Na₂SiO₃-activated geopolymer achieved a maximum compressive strength of 26.33 MPa. The superior strength of VAGPM with NaOH activator solution could be attributed to the smaller ionic size of sodium ions, rendering it more active than potassium ions, thereby facilitating better dissolution of the source material, leading to more oligomers formation than in VAGPM with KOH activator solution [45,81,82]. Although the potassium ion's higher basicity makes it easier for surface silanol groups to ionise, the rate at which silica dissolves depends on how well the cations are hydrated. Considering that sodium ions have a higher charge density than potassium ions, their stronger hydration causes them to release more energy [83]. Research conducted by Sore et al. [84] linked the superior compressive strength of NaOH-activated Geopolymer, in comparison to KOH specimens, to the reduced porosity and higher crystallinity of the NaOH-activated Geopolymer. The observed superior compressive strength of NaOH-activated Geopolymer appears to align with previous research studies on geopolymers [23,36,85,86].

3.3. The Geopolymer Response to Elevated Temperatures

3.3.1. Compressive and Residual Compressive Strengths

The compressive strength results of the VAGPM specimens with and without CNS before and after exposure to various temperature levels and durations are shown in Figures 10 and 12 for NaOH-Na₂SiO₃ and Figures 11 and 13 for KOH-Na₂SiO₃ geopolymers, with 1-hour and 2-hour durations of exposure. Regardless of the CNS replacement level, the activation method and the duration, the compressive strengths of the VAGPM specimens displayed an increase up to a temperature level of 600°C, apart from NaOH-Na₂SiO₃

activated geopolymers exposed to 600°C for 2 hours and all the specimens subject to the elevated temperature of 800°C, which experienced a substantial reduction in their compressive strengths. The compressive strength for NS0 increased by 1.1%, 7.0% and 1.5% when exposed to 200, 400 and 600 for 1 hour, respectively. Conversely, the compressive strength for KSO rose by 2.7%, 4.5%, and 6.3% after the samples were exposed to 200, 400, and 600°C, respectively, for 1 hour. The compressive strength of NS0 increased by 2.0%, 12.8% and reduced by 4.4%, while the compressive strength for KSO increased by 7.7%, 13.1% and 8.1% for 200, 400 and 600°C, respectively, when the exposure duration was increased to 2 hours for both geopolymers.

The VA mortar containing CNS showed a similar compressive strength behaviour with increasing temperature. For CNS levels 1 to 5%, the compressive strength improved with rising temperature up to 600°C, with the maximum compressive strength improvement being recorded for both NS2 and KS2. The compressive strength for NS2 was increased by 5.0%, 9.3% and 4.3%, while for KS2, strength was increased by 4.1%, 10.9% and 2.5%, after exposure to 200, 400 and 600°C, respectively, for 1 hour. On increasing the exposure duration to 2hrs, the compressive strength for NS2 increased by 8.5%, 13.0% but reduced by 0.62%, while for KS2, strength was increased by 5.34%, 15.7% and 6.76%, for 200, 400 and 600°C, respectively, for both geopolymers.

NS1, NS3, NS4, and NS5 experienced a maximum improvement in the compressive strength by 9.5%, 9.7%, 11.3% and 8.1%, while KS1, KS3, KS4 and KS5 experienced a maximum gain in the compressive strength by 17.7%, 14.8%, 10% and 12.1% all recorded at 400°C. The recorded superior residual compressive strength values for NS2 and KS2 may have followed the improvement in compressive strength recorded at ambient temperature conditions. The improved residual strength of the specimens with 2% colloidal nanosilica indicated that 2% CNS was the optimum replacement level. The reduced improvement in the residual strength with colloidal nanosilica content beyond 2% in the geopolymer may have been due to the agglomeration of the nanoparticles, thus preventing uniform dispersion [36]. The observed improvement in the remaining compressive strength with increasing temperature up to 600°C in this study points out improved high-temperature resistance, a behaviour that can be linked to the filling effect, and the increased silica nanoparticles reactivity in the skeleton of the geopolymer matrix [1,3]. Additionally, the residual compressive strength increase could be credited to promoted polycondensation between the chain-like geopolymer gels [5,87,88]. Thus, the current study further confirms that the optimum CNS replacement level is 2% for volcanic ash (VA) locally sourced in Kenya. While KOH-Na₂SiO₃ geopolymers exhibited lower compressive strengths at ambient temperature when compared to NaOH-Na₂SiO₃ geopolymers, it was noted that KOH-Na₂SiO₃ geopolymers demonstrated a consistently higher

percentage of strength increase and retention across all CNS content levels when subjected to elevated temperatures, as opposed to NaOH-Na₂SiO₃ geopolymers. The observed phenomenon seems to agree with previous research studies. It is attributed to the densified geopolymer matrix and the decrease in the pore sizes, which is beneficial to strength improvement [36,71].

On a further rise in temperature up to 800°C for the 1- and 2-hour exposure duration, a decline in the residual compressive strengths was recorded in all the specimens, both with and without CNS. The residual compressive strength of NS0 reduced to just 69.5% of the ambient temperature compressive strength while the compressive strength for KS0 reduced to 72.2% after exposure to 800°C respectively for 1 hour. When the duration of exposure was extended to 2 hours, the compressive strength of NS0 reached 66.1%, while for KS0, it dropped to 72.0%. The VA mortar containing CNS showed a similar compressive strength behaviour with increasing temperature. NS1, NS2, NS3, NS4 and NS5 retained 63.6%, 71.1%, 81.8%, 80.5% and 74.5% of the initial compressive strength, while KS1, KS2, KS3, KS4 and KS5 retained 77.9%, 87.4%, 75.8%, 85.1% and 77.3% when they were exposed to 800°C for 1 hour.

Increasing the exposure duration to 2 hours while maintaining the temperature at 800°C seemed to have little effect on the remaining compressive strength of the KOH-Na₂SiO₃ VA geopolymers. On increasing the exposure duration to 2 hours with the temperature level of 800°C, the NaOH-Na₂SiO₃ specimens experienced a further reduction in the residual compressive strength with NS1, NS2, NS3, NS4 and NS5 retaining 58.9%, 63.0%, 69.9%, 78.1% and 70.0% of the initial compressive strength.

These results indicate that the KOH-Na₂SiO₃ geopolymer specimens are relatively stable at elevated temperatures compared to NaOH-Na₂SiO₃ specimens at 800°C. Another significant observation was that silica nanoparticles increased the retained compressive strengths of the geopolymer specimens. However, the increase in the CNS level was observed to have an irregular effect regarding the residual compressive strengths at 800°C.

At 800°C, the increase in the specimen paste shrinkage may have led to the decreased compressive strengths of the geopolymer [89]. Another reason for the decrease in the compressive strengths might have been due to the deterioration of the paste and the aggregate bonds resulting from paste contracting while aggregates expanded [33,35,88]. The enhancement of the residual compressive strength of the specimens with CNS compared to the reference specimens at increased temperatures may have been due to an improvement in the bonds between the paste and the aggregates. Previous research studies also reported dropping compressive strengths at high temperatures [2,36,90].

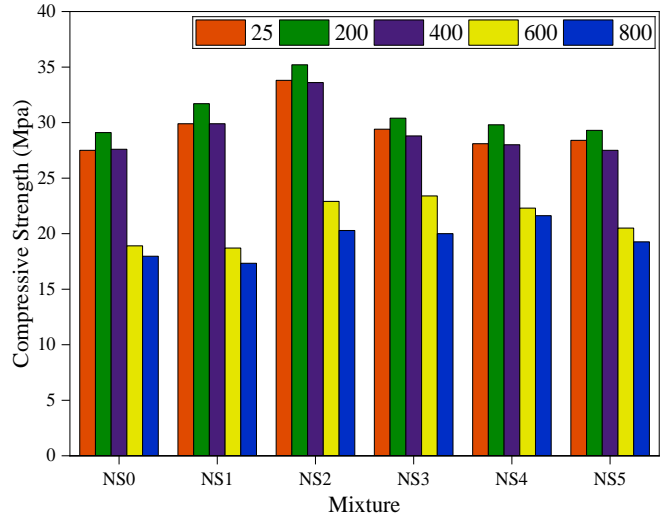


Fig. 10 Compressive and residual compressive strengths of NaOH-Na₂SiO₃ activated mortar with and without CNS (1hr)

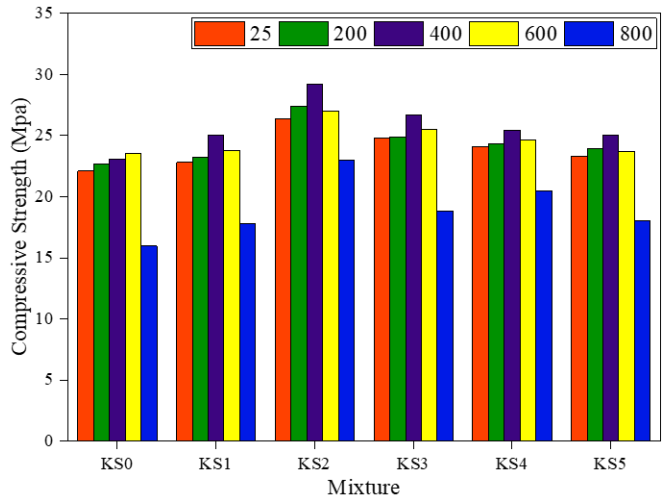


Fig. 11 Compressive and residual compressive strengths of KOH-Na₂SiO₃ activated mortar with and without CNS (1hr)

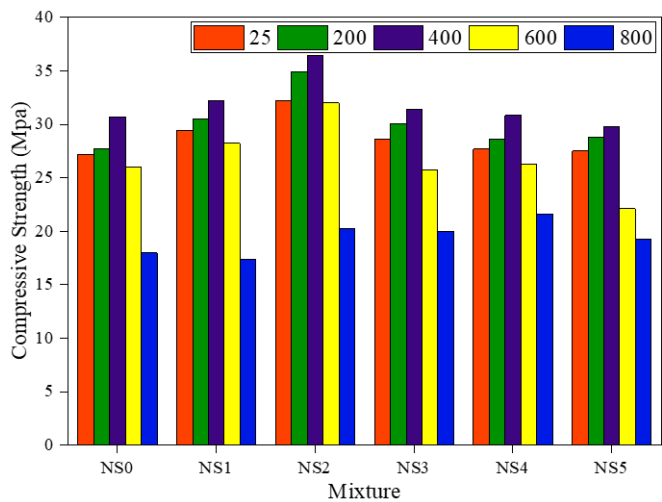


Fig. 12 Compressive and residual compressive strengths of NaOH-Na₂SiO₃ activated mortar with and without CNS (2hr)

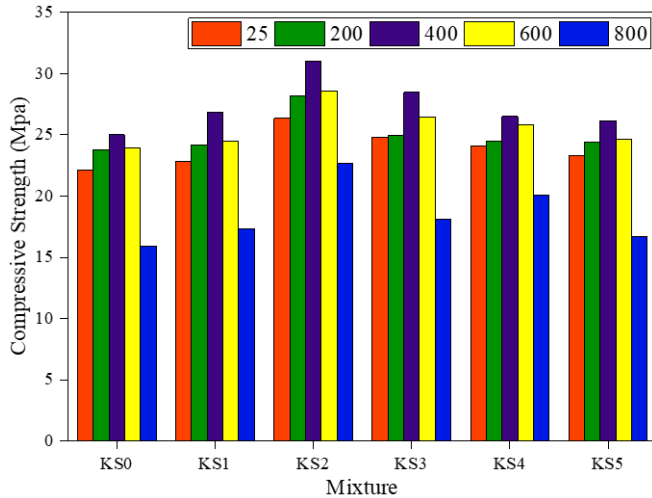


Fig. 13 Compressive and residual compressive strengths of KOH- Na_2SiO_3 activated mortar with and without CNS (2hr)

3.3.2. Mass Loss

Mass loss was calculated as the percentage decrease in mass after exposure to elevated temperatures relative to the initial mass of the specimen. Figures 14 (a) and (b) and Figures 15 (a) and (b) illustrate the mass loss findings for VAGPM specimens, both with and without CNS, after exposure to elevated temperatures. The geopolymer specimens experienced a continuous mass loss of up to 800°C. The mass losses of the NS0 specimens were approximately 1.65%, 2.9%, 4.4% and 6.6% when exposed to high temperatures of 200°C, 400°C, 600°C and 800°C, respectively, for 1hr. When the duration of exposure for the same temperature levels was increased to 2hrs, NS0 showed approximate mass losses of 2.3%, 3.2%, 5.34% and 6.9%. KS0 showed mass losses of 1.41%, 2.44%, 4.2% and 5.9% for 1hr and 1.85%, 3.0%, 4.7% and 6.2% for 2hrs duration of exposure to elevated temperatures 200°C, 400°C, 600°C and 800°C respectively. Water evaporation and dihydroxylation have been reported to be the two processes triggering the reduction in mass of the geopolymers under elevated temperatures [71]. The decrease in mass at elevated temperatures has been linked to the evaporation of the free water in the specimen pores at temperatures below 100°C, water chemically bonded within the gel pores at temperatures between 100 and 300°C and finally, hydroxyl groups which vaporize when temperatures exceed 300°C [25,71]. Additionally, the reduction in mass of the geopolymer samples at 800°C may have been due to the breakdown of the geopolymer structure compounds [25]. From the mineralogical investigation of the mortar specimens using XRD in Figures 16 and 17, hydroxysodalite was observed in geopolymers at ambient temperature and may have contributed to mass loss as it has been reported by Lemougna et al. [91] that hydroxysodalite is known to lose weight continuously from 100°C to 800°C practically. The impact of the CNS on mass losses of the NaOH- Na_2SiO_3 and KOH- Na_2SiO_3 geopolymers showed that mass loss in VAGPM specimens with CNS was less than the mass loss of

the reference VAGPM specimens for all the temperature levels and durations. The maximum mass losses at 800°C for the NS1, NS2, NS3, NS4 and NS5 were 5.48%, 5.15%, 5%, 4.7% and 4.3% of the ambient temperature mass, respectively, while for the KS1, KS2, KS3, KS4 and KS5 they were 5.3%, 4.9%, 4.2%, 3.4% and 3% respectively with the exposure duration of 1 hour. When the duration of exposure was extended to 2 hours while maintaining the level of temperature at 800°C, the mass losses for the NS1, NS2, NS3, NS4 and NS5 were 6.1%, 5.7%, 5.8%, 5.2% and 4.6% while for the KS1, KS2, KS3, KS4 and KS5 they were 5.8%, 5.4%, 5.1%, 4.68% and 4.4% respectively. The mass losses were reduced with increasing CNS replacement levels. NS5 and KS5 recorded the least mass losses in each activation method.

This outcome can be attributed to the nanosilica having a high specific surface area that led to greater pozzolanic reactivity [92]. Additionally, it was noted that the reduction in mass of NaOH- Na_2SiO_3 geopolymers was slightly higher compared with KOH- Na_2SiO_3 geopolymers with or without CNS. The result indicates that VAGPM specimens produced with KOH- Na_2SiO_3 have higher thermal stability at high temperatures than NaOH- Na_2SiO_3 geopolymers. In specimens that utilise Na-containing activators, the breakdown appears to occur more quickly after firing. The rapid deterioration could be a result of sodium ions exhibiting a higher diffusion coefficient compared to potassium ions in the geopolymer matrix upon firing [47,93]. Increasing the exposure duration from 1 hour to 2 hours increased elevated temperature degradation of the hardened geopolymer samples for all the temperature levels. The findings suggest that, aside from the heating temperature, the heating time of the geopolymer specimens is a crucial factor relating to the properties of the geopolymers [71,94].

3.3.3. Volumetric Changes

Volume changes in geopolymers can indicate the fundamental response that triggers failure in a fire [94]. The volumetric changes of the test specimens after being exposed to different temperature levels are illustrated in Figures 16 (a) and (b) and Figures 17 (a) and (b). The findings indicated that higher volumetric stability was prominent in the specimens enriched with CNS, thus showing less shrinkage. The observed reduction in the volume change with increased CNS levels can be attributed to the filling of nanopores by the CNS, thus improving fire resistance. In the temperature ranges from ambient to the maximum 800°C, all geopolymer specimens showed a similar trend in the volume changes, although with a varying degree of change. The initial reduction in the volume of the specimens from ambient temperature to 400°C and 600°C can be attributed to geopolymer structure densification [95], evaporation of the unbonded water in the pores at temperatures below 100°C, chemically bonded water in the gel pores at temperatures between 100 and 300°C and finally the hydroxyl groups which have been reported to evaporate at temperatures exceeding 300°C [25,71].

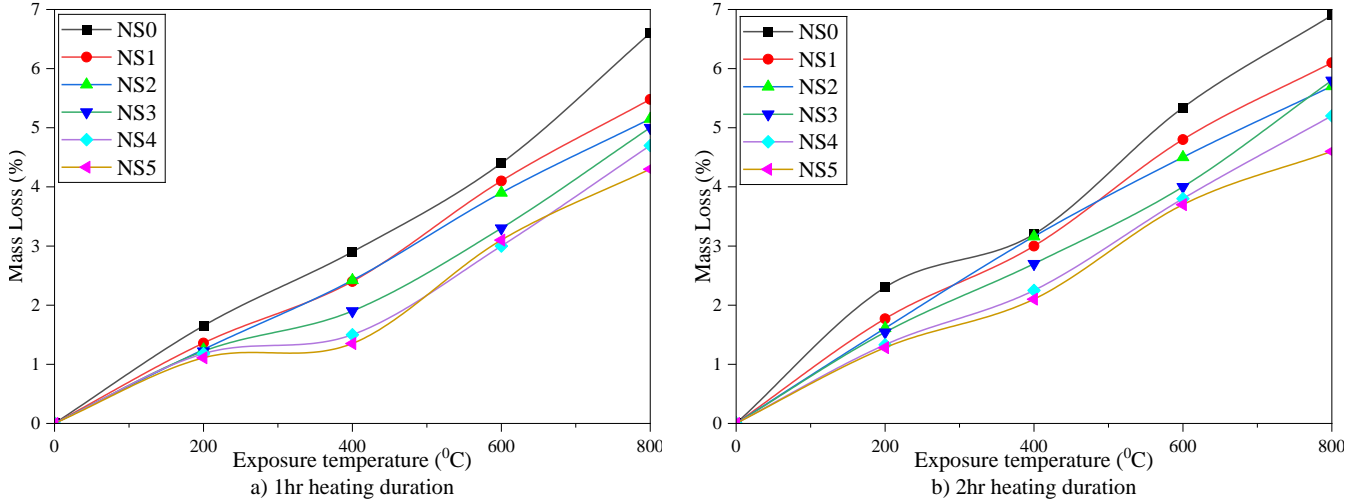


Fig. 14 Mass loss of NaOH-Na₂SiO₃ geopolymers after elevated temperatures

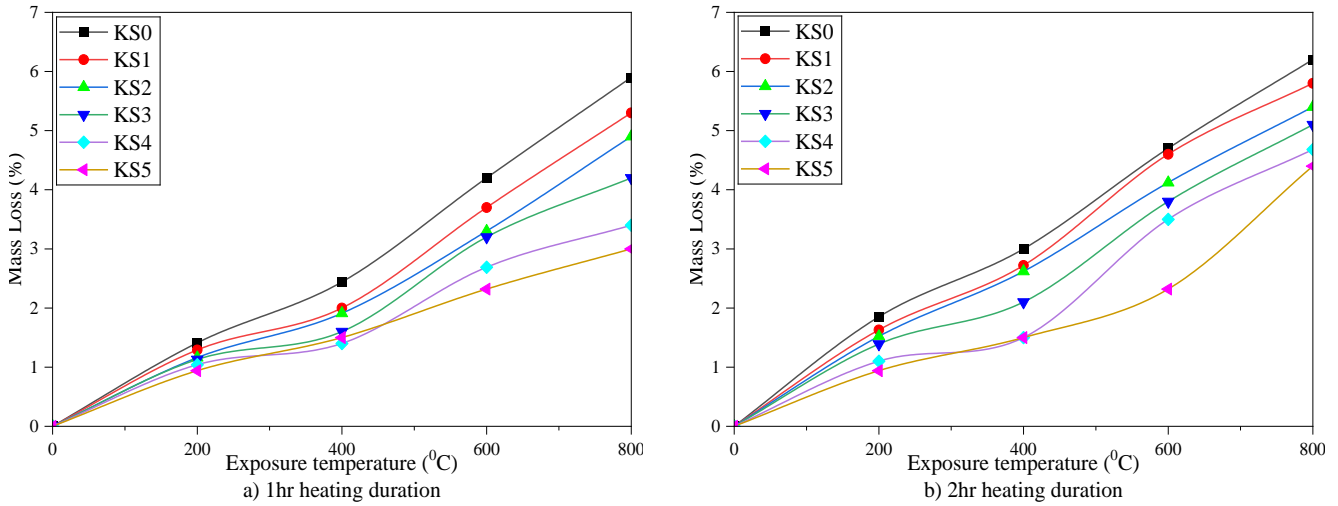


Fig. 15 Mass loss of KOH-Na₂SiO₃ geopolymers after elevated temperatures

A sharp decrease in volume was recorded when the temperature was increased from 600°C to 800°C, and this may have brought about the residual compressive strength decline recorded in Figures 10, 11, 12, and 13. NS0 was characterised by a volumetric reduction of 2.66%, 2.78%, 3.25% and 3.58%, while KS0 achieved 2.19%, 2.3%, 3% and 3.33% reduction in volume at 200, 400, 600 and 800°C temperature levels, respectively, for an exposure duration of 1 hour. When the exposure duration was extended to 2 hours, NS0 achieved 2.69%, 2.84%, 3.53% and 3.99%, while KS0 achieved 2.55%, 2.69%, 3.11% and 3.47% reduction in volume for the same temperature levels. At 200°C, the NaOH-Na₂SiO₃ and KOH-Na₂SiO₃ geopolymers specimens with varying CNS levels were characterised by a volume shrinkage of up to 2.51% and 2.14% for 1 hour and 2.75% and 2.33% for 2 hours respectively. At 400°C, the NaOH-Na₂SiO₃ and KOH-Na₂SiO₃ geopolymers specimens with varying CNS levels were characterised by a volumetric shrinkage of up to 2.77% and 2.27% for 1 hour and 2.81% and 2.48% for 2 hours respectively. At 600°C, the NaOH-Na₂SiO₃ and KOH-

Na₂SiO₃ geopolymers specimens with varying CNS levels were characterised by a volume shrinkage of up to 2.96% and 2.89% for 1 hour and 3.04% and 2.91% for 2 hours respectively.

The volume reductions at 800°C for the NS1, NS2, NS3, NS4 and NS5 were 3.41%, 3.23%, 3.04%, 2.94% and 2.8% of the ambient temperature mass, respectively, while for the KS1, KS2, KS3, KS4 and KS5 they were 3.16%, 3.05%, 2.9%, 2.72% and 2.71% respectively with the exposure duration of 1 hour. When the exposure duration was increased to 2hrs while maintaining the level of temperature at 800°C, the mass losses for the NS1, NS2, NS3, NS4 and NS5 were 3.95%, 3.71%, 3.52%, 3.01% and 2.96% while for the KS1, KS2, KS3, KS4 and KS5 they were 3.21%, 3.14%, 2.96%, 2.83% and 2.75% respectively. At all temperatures, it was observed that the KOH-Na₂SiO₃ geopolymers specimens displayed a slightly lower volume shrinkage than its NaOH-Na₂SiO₃ counterpart, a trend also reported in the previous studies [36,96].

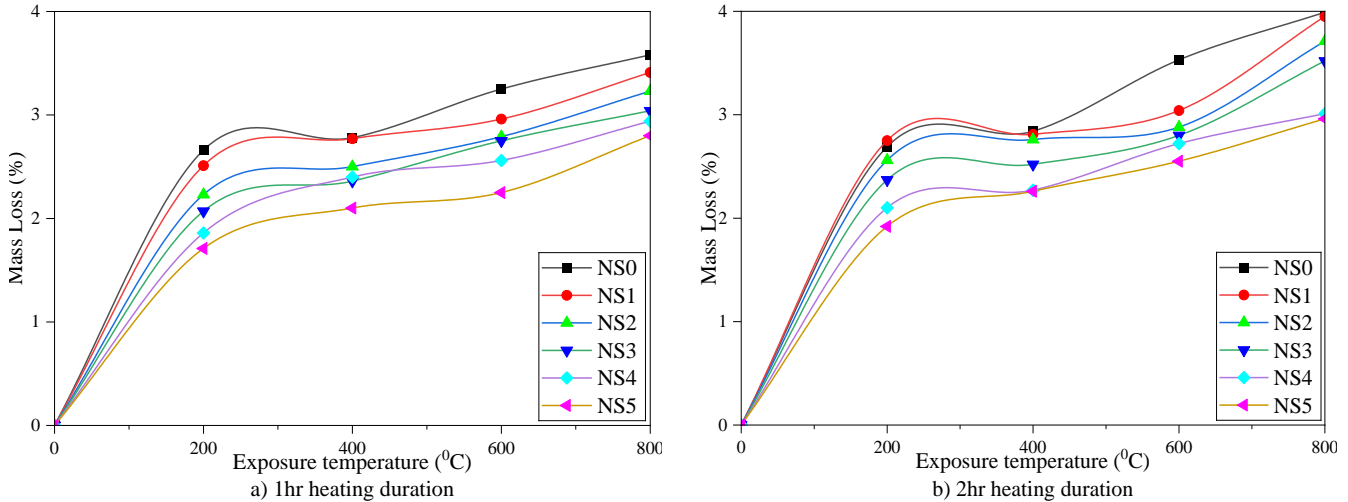


Fig. 16 Volume changes for NaOH-Na₂SiO₃ geopolymer with varying CNS levels

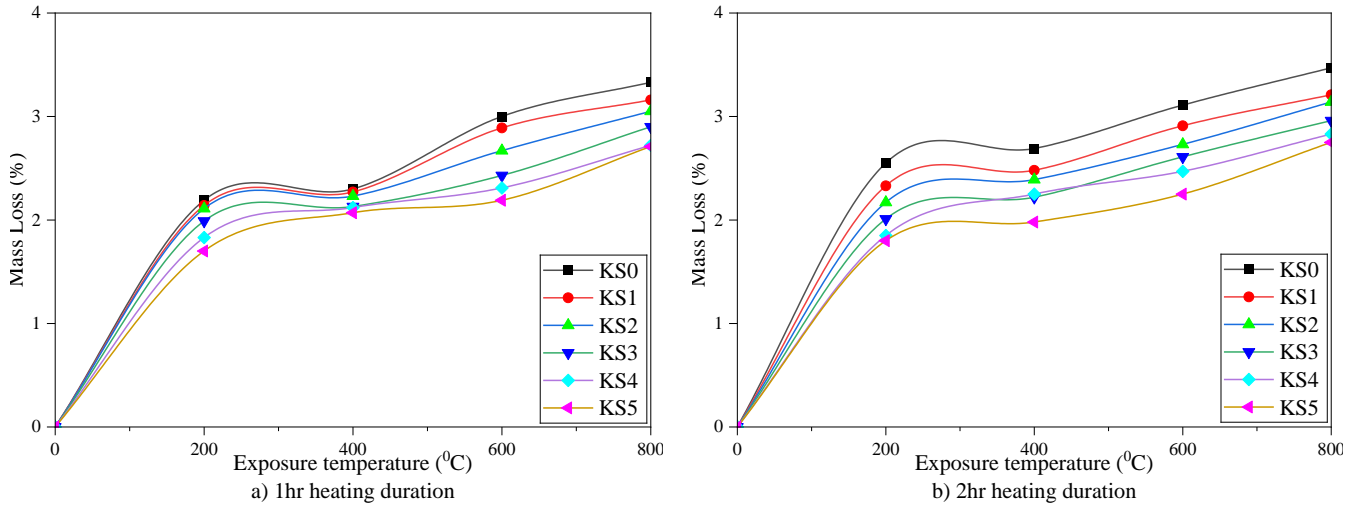


Fig. 17 Volume changes for KOH-Na₂SiO₃ geopolymer with varying CNS levels

3.3.4. Visual Analysis of the Specimens

The appearance of pre- and post-exposure to elevated temperatures for control and optimum colloidal nanosilica level specimens with changing exposure durations for both geopolymer activation methods are presented in Figure 18. The changes due to elevated temperatures were captured after carefully examining the specimens pre- and post-exposure to the soaring temperatures. Prior to exposing the specimens to the high temperatures, the specimens were generally dark greyish. After subjecting the geopolymer mortar samples to a temperature level of 200°C for 1 and 2 hours, the colour turned lighter and had a greyish tinge compared with the ambient temperature specimens. The specimens were observed to turn light greyish with faint beige colouration on increasing the temperature to 400°C. At 600°C and 800°C, the specimens turned pinkish/reddish brown. The KOH-Na₂SiO₃ geopolymer specimens were well preserved without cracks up to 800°C, while some NaOH-Na₂SiO₃ geopolymer specimens displayed tiny hairline cracks at 800°C. Notably, all the geopolymer specimens subject to temperatures up to 800°C

maintained their cubic shapes and presented no explosive spalling or bursting phenomenon. The tiny hairline cracks observed could be due to the thermal incompatibility between the aggregates and the binder paste [50], the dehydration of the binder paste, the release of free water in the binder paste, and the disintegration of the geopolymer microstructure caused by the elevated temperatures [53]. The observed colour changes in specimens at elevated temperatures may have been caused by the considerably high Fe₂O₃ content in the ash and the subsequent oxidation of the iron particles at temperatures of 600°C and 800°C [52,89].

Additionally, the colour change could be attributed to the evaporating water molecules from the geopolymer matrix structure [7]. The mortar specimens were more identical regarding the temperature level and exposure duration than the chemical composition. In fact, the variation in both the activating solution and the level of colloidal nanosilica replacement exhibited a marginal impact on the colours of the specimens across the identical temperature levels of exposure.

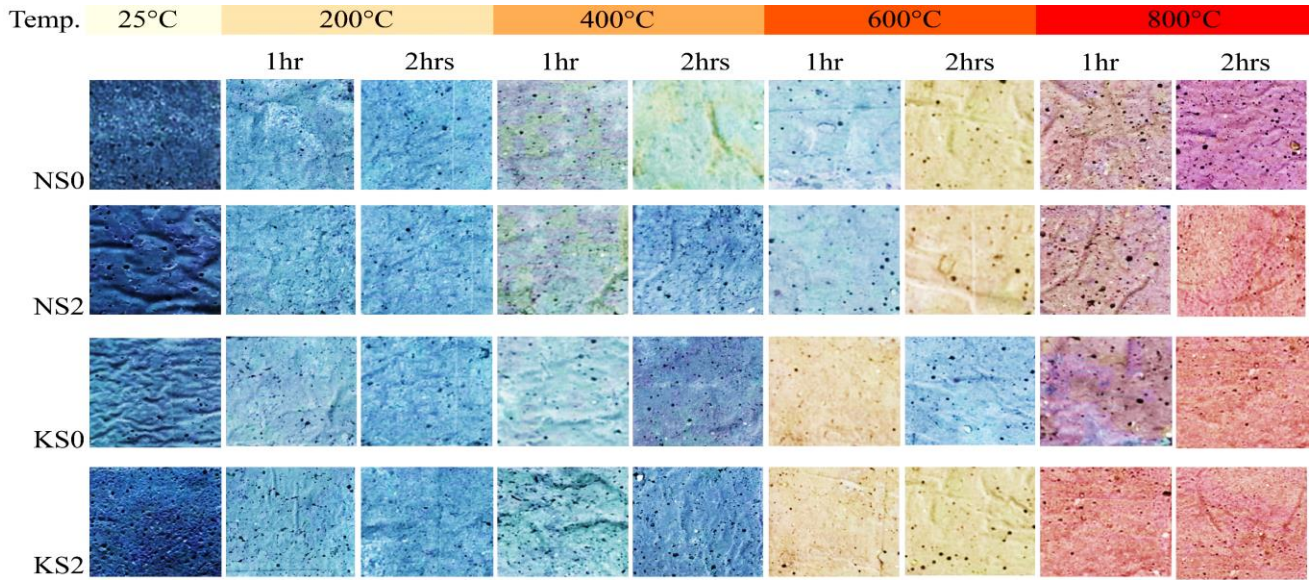


Fig. 18 Visual changes of geopolymer specimens under elevated temperatures

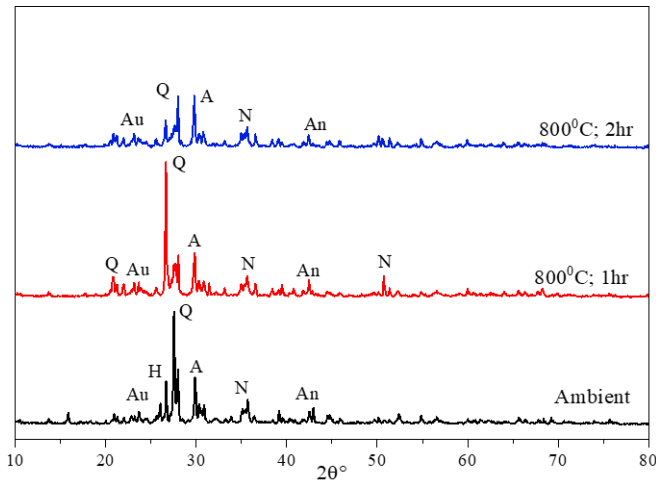


Fig. 19 XRD pattern for NS0

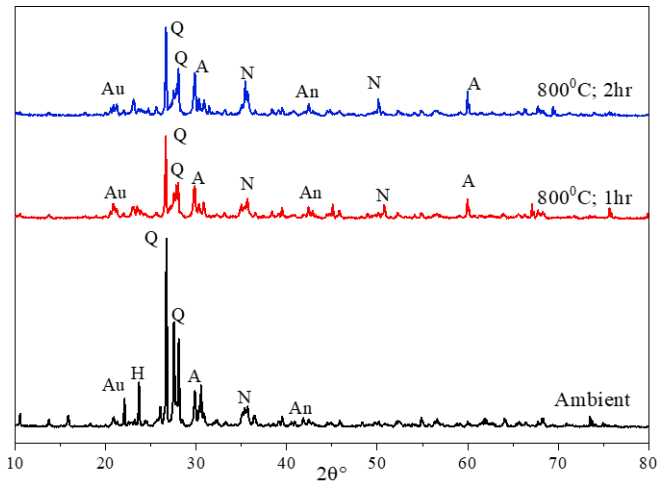


Fig. 20 XRD pattern for NS2

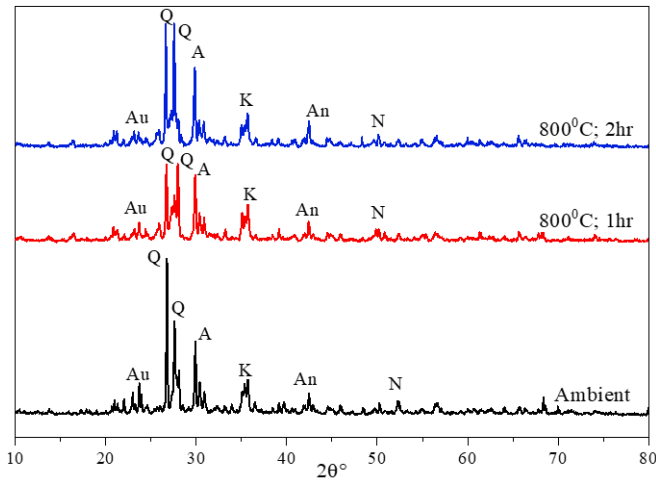


Fig. 21 XRD pattern for KS0

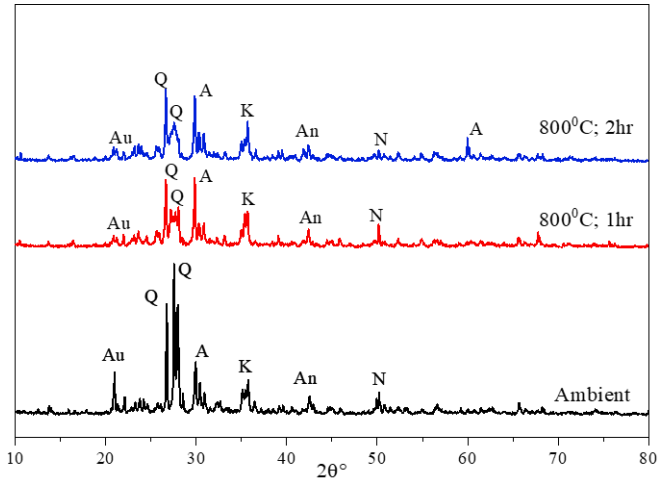


Fig. 22 XRD pattern for KS2

[Note: A: Albite, An: Anorthite, Au: Augite, K: Potassium Aluminium Silicate Hydrate, N: Sodium Aluminium Silicate Hydrate, H: Hydroxysodalite
Q: Quartz]

3.3.5. Microstructural Analysis

The microstructure of the VAGPM specimens was observed through XRD analysis and SEM to assess the impact of the elevated temperatures.

X-ray Diffraction Analysis

The XRD diffractograms of the selected reference and optimum CNS levels for NaOH-Na₂SiO₃ and KOH-Na₂SiO₃ activated geopolymer specimens at room temperature and after high-temperature exposure are shown in Figures 19 to 22. The diffraction patterns of the VAGPM geopolymers showed the existence of a large number of amorphous phases with some crystalline minerals like quartz, hydroxy sodalite and albite even before heating. Other phases included sodium aluminium silicate hydrate in all the geopolymers tested and potassium aluminium silicate hydrate in KS0 and KS2. The newly identified minerals might have resulted from the reaction between the amorphous component of the source material and the alkaline activator solution [97]. The broad peaks of the VAGPM geopolymers matrix were observed in the regions between 25–32 2θ. Some of the phases in the source material, such as maghemite and augite, seemed to have been consumed during geopolymerization. In contrast, others, like anorthite, remained relatively unaltered or partially dissolved.

After the geopolymer specimens were subjected to a temperature of 800°C for both 1 hour and 2 hours,

hydroxysodalite seemed to have disappeared and may have contributed to the mass loss of the geopolymers [91]. It was also observed that there was some substantial reduction in the intensities of some peaks, such as quartz, at elevated temperatures. For all the geopolymers, some initial phases, such as quartz, were maintained at 800°C. Additionally, the appearance of more albite peaks still at 800°C may have contributed to the strength deterioration recorded [25,98]. The CNS in the mix may have contributed to the rise in the quartz phase in the geopolymer matrix [3]. The quartz phase increase improved the residual compressive strength at elevated temperatures [71].

Scanning Electron Microscopy Analysis

The SEM images of the selected control and optimum CNS levels for NaOH-Na₂SiO₃ and KOH-Na₂SiO₃ activated geopolymer specimens at ambient temperature and after high temperatures exposure are shown in Figures 23 to 28. The CNS specimens displayed a relatively more compact microstructure than the control specimens of both activation methods. The SEM images also showed that at 800°C for both 1 and 2 hours, the specimens showed a higher porosity than those at ambient temperature. The arrows on the SEM images show voids/ pores and micro-cracks. The observed voids and micro-cracks may have resulted from the escape of water at elevated temperatures [99]. A relatively loose mortar matrix contributes to the compressive strength decrease recorded [35].

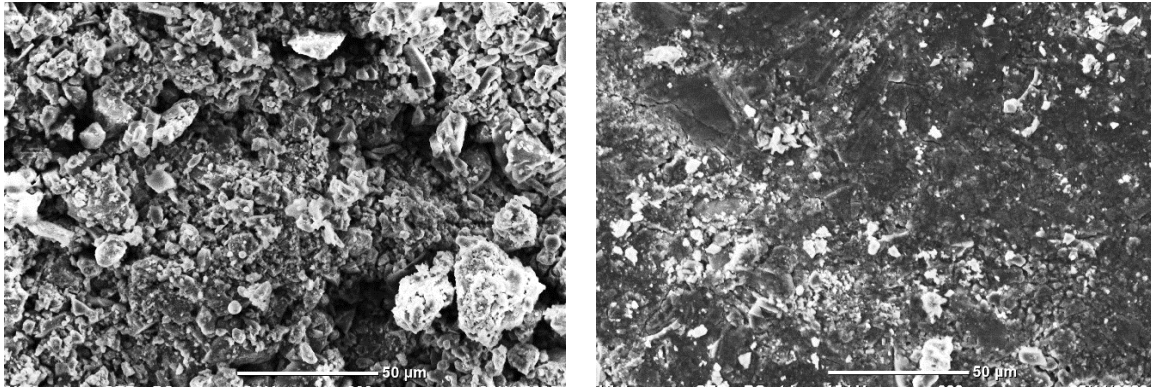


Fig. 23 SEM images of NaOH-Na₂SiO₃ samples; ambient temperature, a) NS0, b) NS2

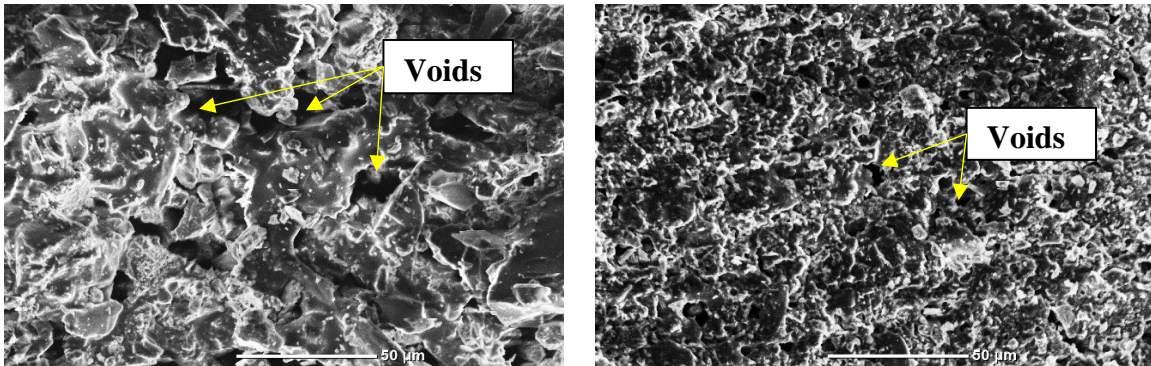


Fig. 24 SEM images of NaOH-Na₂SiO₃ samples at 800°C for 1hr; a) NS0, b) NS2

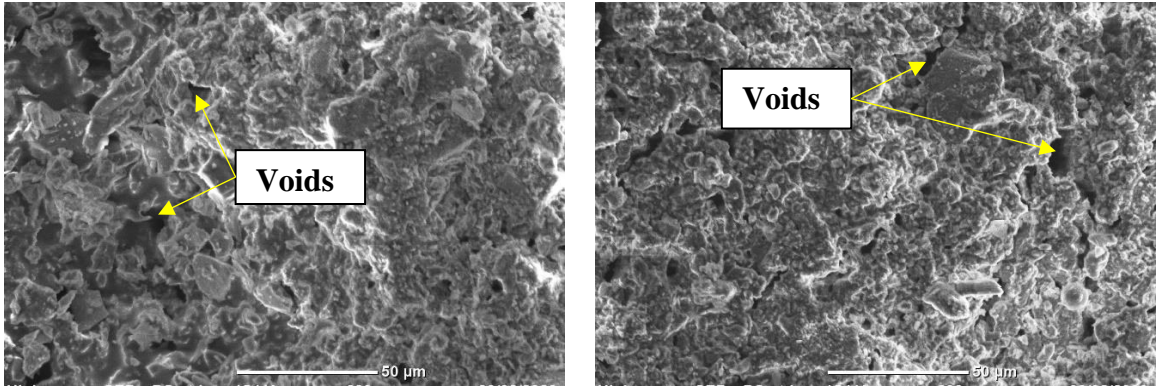


Fig. 25 SEM images of NaOH-Na₂SiO₃ samples at 800°C for 2hr; a) NS0, b) NS2

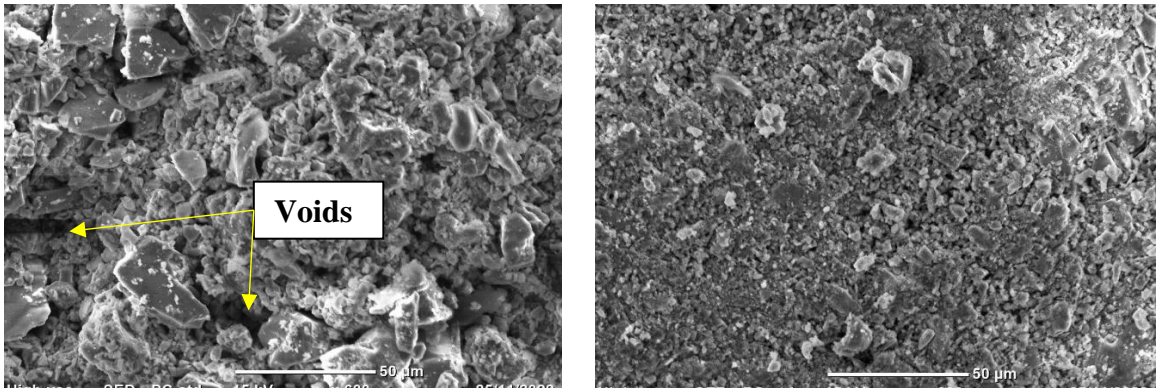


Fig. 26 SEM images of KOH-Na₂SiO₃ samples at ambient temperature; a) KS0, b) KS2

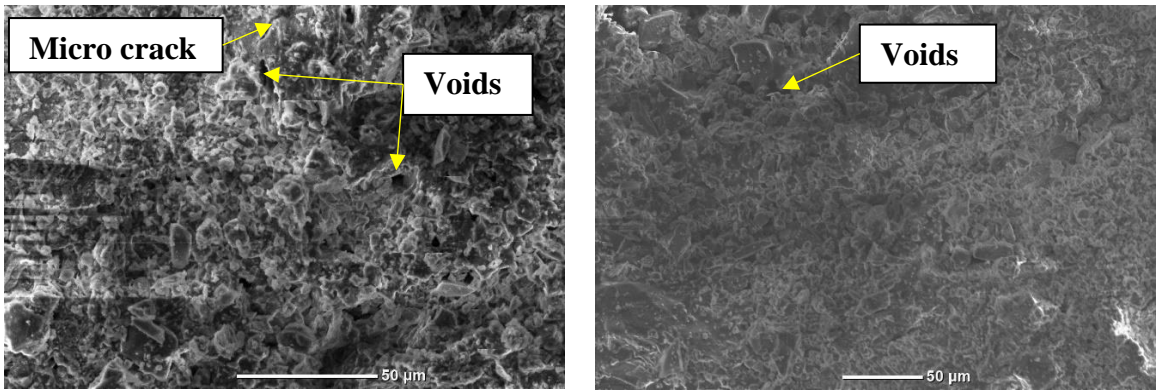


Fig. 27 SEM images of KOH-Na₂SiO₃ samples at 800°C for 1hr; a) KS0, b) KS2

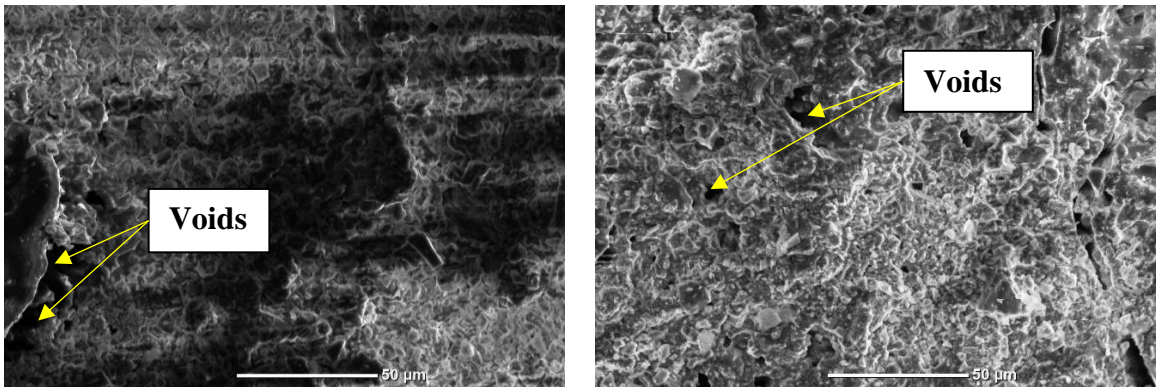


Fig. 28 SEM images of KOH-Na₂SiO₃ samples at 800°C for 2hr; a) KS0, b) KS2

4. Conclusion

In the present study, the impact of colloidal nanosilica on the workability, initial compressive strength, and performance under elevated temperatures of geopolymer mortar derived from Kenyan volcanic ash (VAGPM), and activated using NaOH-Na₂SiO₃ and KOH-Na₂SiO₃ alkaline solutions, has been examined. The conclusions drawn from the conducted experimental tests and the analysed data in this study are as follows:

1. Incorporating Colloidal Nanosilica (CNS) in the VAGPM resulted in a reduction of the workability of the mixes for both NaOH-Na₂SiO₃ and KOH-Na₂SiO₃ activated geopolymers. This reduction was ascribed to the silica nanoparticles having a high specific surface area, leading to higher water demand and a subsequent decline in mortar flow. The flow values are reduced with increasing CNS content.
2. The flowability of VAGPM mixes with KOH-Na₂SiO₃ alkaline activator was higher than that of the VAGPM mixes activated with NaOH-Na₂SiO₃, regardless of the presence of CNS.
3. The optimal replacement was observed at 2% colloidal nanosilica, significantly improving compressive strength. Higher CNS content (3%, 4%, and 5%) contributed insignificantly to the compressive strength of the geopolymer specimens both pre- and post-exposure to elevated temperatures. The enhancement in the compressive strength was attributed to CNS providing additional active nucleation sites, introducing a nano-filling effect, enhancing the pozzolanic reaction, and contributing to geopolymer microstructure densification.
4. All NaOH-Na₂SiO₃ activated mixtures exhibited improved compressive strength up to 400°C, while KOH-Na₂SiO₃ activated mixtures displayed slight improvement up to 600°C, indicating enhanced polycondensation between chain-like geopolymer gels.
5. Despite lower ambient and elevated temperature compressive strengths in KOH-Na₂SiO₃ VA geopolymers

compared to NaOH-Na₂SiO₃ VA geopolymers, the former showed higher percentage strength increase and retention when subjected to elevated temperatures. This suggests that the VA geopolymer's compressive strength behaviour is affected by the nature of the activating alkali hydroxide.

6. VAGPM specimens containing the KOH-Na₂SiO₃ activator exhibited lower mass loss and volume shrinkage compared to the VAGPM specimens activated with NaOH-Na₂SiO₃.
7. Prior to the elevated temperatures exposure, the VAGPM specimens appeared dark greyish, then turned to lighter and greyish tinge at 200°C, light greyish with faint beige colouration at 400°C, and finally pinkish/reddish brown at 600°C and 800°C.
8. Quartz mineral was detected in all the VAGPM samples both before and after being exposed to elevated temperatures. The addition of the CNS seemed to have increased the quartz phase in the geopolymer matrix. Others, like hydroxysodalite, seemed to have disappeared after exposure to the 800°C for 1 and 2 hours. CNS yielded a denser microstructure.

These findings contribute valuable insights into the effect of CNS on volcanic ash-based geopolymer behaviour before and after exposure to elevated temperatures.

Funding Statement

The research was funded by the African Union through the Pan African University Institute for Basic Sciences, Technology and Innovation (PAUSTI).

Acknowledgements

The authors wish to extend their heartfelt thanks to the Pan African University for their generous support in facilitating this research. Furthermore, they would like to convey their sincere appreciation to the Jomo Kenyatta University of Agriculture and Technology for the provision of laboratory equipment crucial to the success of this study.

References

- [1] Rahel Kh. Ibrahim, R. Hamid, and M.R. Taha, "Fire Resistance of High-Volume Fly Ash Mortars with Nanosilica Addition," *Construction and Building Materials*, vol. 36, pp. 779-786, 2012. [[CrossRef](#)] [[Google Scholar](#)] [[Publisher Link](#)]
- [2] M.W. Hussin et al., "Performance of Blended Ash Geopolymer Concrete at Elevated Temperatures," *Materials and Structures*, vol. 48, pp. 709-720, 2014. [[CrossRef](#)] [[Google Scholar](#)] [[Publisher Link](#)]
- [3] Alaa M. Rashad, and Ahmed S. Ouda, "Thermal Resistance of Alkali-Activated Metakaolin Pastes Containing Nano-Silica Particles," *Journal of Thermal Analysis and Calorimetry*, vol. 136, pp. 609-620, 2018. [[CrossRef](#)] [[Google Scholar](#)] [[Publisher Link](#)]
- [4] Salmabanu Luhar, Sandeep Chaudhary, and Ismail Luhar, "Thermal Resistance of Fly Ash Based Rubberized Geopolymer Concrete," *Journal of Building Engineering*, vol. 19, pp. 420-428, 2018. [[CrossRef](#)] [[Google Scholar](#)] [[Publisher Link](#)]
- [5] Siti Nooriza Abd Razak et al., "Fire Performance of Fly Ash-Based Geopolymer Concrete: Effect of Burning Temperature," *IOP Conference Series: Earth and Environmental Science*, 4th International Symposium on Green and Sustainable Technology, Kampar, Malaysia, vol. 945, pp. 1-6, 2021. [[CrossRef](#)] [[Google Scholar](#)] [[Publisher Link](#)]
- [6] S.K. Saxena, Mukesh Kumar, and N.B. Singh, "Fire Resistant Properties of Alumino Silicate Geopolymer Cement Mortars," *Materials Today: Proceedings*, vol. 4, no. 4, pp. 5605-5612, 2017. [[CrossRef](#)] [[Google Scholar](#)] [[Publisher Link](#)]
- [7] Marouane EL Alouani et al., "Influence of the Nature and Rate of Alkaline Activator on the Physicochemical Properties of Fly Ash-Based Geopolymers," *Advances in Civil Engineering*, vol. 2020, pp. 1-13, 2020. [[CrossRef](#)] [[Google Scholar](#)] [[Publisher Link](#)]

- [8] Sujay Chetan Nanavati et al., “A Review on Fly Ash Based Geopolymer Concrete,” *IOSR Journal of Mechanical and Civil Engineering*, vol. 14, no. 4, pp. 12-16, 2017. [[Google Scholar](#)] [[Publisher Link](#)]
- [9] Rafael Andres Robayo-Salazar, Mejía de Gutiérrez, and Francisca Puertas, “Study of Synergy between a Natural Volcanic Pozzolan and a Granulated Blast Furnace Slag in the Production of Geopolymeric Pastes and Mortars,” *Construction and Building Materials*, vol. 157, pp. 151-160, 2017. [[CrossRef](#)] [[Google Scholar](#)] [[Publisher Link](#)]
- [10] Enes Ekinci et al., “The Improvement of Mechanical, Physical and Durability Characteristics of Volcanic Tuff Based Geopolymer Concrete by Using Nano Silica, Micro Silica and Styrene-Butadiene Latex Additives at Different Ratios,” *Construction and Building Materials*, vol. 201, pp. 257-267, 2019. [[CrossRef](#)] [[Google Scholar](#)] [[Publisher Link](#)]
- [11] Salmabanu Luhar, Demetris Nicolaidis, and Ismail Luhar, “Fire Resistance Behaviour of Geopolymer Concrete: An Overview,” *Buildings*, vol. 11, no. 3, pp. 1-29, 2021. [[CrossRef](#)] [[Google Scholar](#)] [[Publisher Link](#)]
- [12] Nikolaos Nikoloutsopoulos et al., “Physical and Mechanical Properties of Fly Ash Based Geopolymer Concrete Compared to Conventional Concrete,” *Buildings*, vol. 11, no. 5, pp. 1-14, 2021. [[CrossRef](#)] [[Google Scholar](#)] [[Publisher Link](#)]
- [13] Alaa M. Rashad, and Sayieda R. Zeedan, “The Effect of Activator Concentration on the Residual Strength of Alkali-Activated Fly Ash Pastes Subjected to Thermal Load,” *Construction and Building Materials*, vol. 25, no. 7, pp. 3098-3107, 2011. [[CrossRef](#)] [[Google Scholar](#)] [[Publisher Link](#)]
- [14] M.S. Morsy et al., “Behavior of Blended Cement Mortars Containing Nano-Metakaolin at Elevated Temperatures,” *Construction and Building Materials*, vol. 35, pp. 900-905, 2012. [[CrossRef](#)] [[Google Scholar](#)] [[Publisher Link](#)]
- [15] Rabii Hattaf et al., “Influence of the Integration of Geopolymer Wastes on the Characteristics of Binding Matrices Subjected to the Action of Temperature and Acid Environments,” *Polymers*, vol. 14, no. 5, pp. 1-19, 2022. [[CrossRef](#)] [[Google Scholar](#)] [[Publisher Link](#)]
- [16] Fatih Kantarci, İbrahim Türkmen, and Enes Ekinci, “Improving Elevated Temperature Performance of Geopolymer Concrete Utilizing Nano-Silica, Micro-Silica and Styrene-Butadiene Latex,” *Construction and Building Materials*, vol. 286, 2021. [[CrossRef](#)] [[Google Scholar](#)] [[Publisher Link](#)]
- [17] Surendra P. Shah, Pengkun Hou, and Maria S. Konsta-Gdoutos, “Nano-Modification of Cementitious Material: Toward a Stronger and Durable Concrete,” *Journal of Sustainable Cement-Based Materials*, vol. 5, no. 1-2, pp. 1-22, 2016. [[CrossRef](#)] [[Google Scholar](#)] [[Publisher Link](#)]
- [18] Jean Noël Yankwa Djobo et al., “Volcanic Ash-Based Geopolymer Cements/Concretes: The Current State of the Art and Perspectives,” *Environmental Science and Pollution Research*, vol. 24, pp. 4433-4446, 2016. [[CrossRef](#)] [[Google Scholar](#)] [[Publisher Link](#)]
- [19] Muhammad Zahid et al., “Statistical Modeling and Mix Design Optimization of Fly Ash Based Engineered Geopolymer Composite Using Response Surface Methodology,” *Journal of Cleaner Production*, vol. 194, pp. 483-498, 2018. [[CrossRef](#)] [[Google Scholar](#)] [[Publisher Link](#)]
- [20] Senthil P. Mathew, A. Sujatha, and Yashida Nadir, “Bond Strength Properties of Confined and Unconfined Coconut Shell Aggregate Concrete by Beam Splice Test,” *Sustainability, Agri, Food and Environmental Research*, vol. 10, pp. 31-34, 2022. [[CrossRef](#)] [[Google Scholar](#)] [[Publisher Link](#)]
- [21] Nabila Shehata et al., “Geopolymer Concrete as Green Building Materials: Recent Applications, Sustainable Development and Circular Economy Potentials,” *Science of the Total Environment*, vol. 836, 2022. [[CrossRef](#)] [[Google Scholar](#)] [[Publisher Link](#)]
- [22] Hengels Castillo et al., “Factors Affecting the Compressive Strength of Geopolymers: A Review,” *Minerals*, vol. 11, no. 12, pp. 1-28, 2021. [[CrossRef](#)] [[Google Scholar](#)] [[Publisher Link](#)]
- [23] Anwar Hosan, Sharany Haque, and Faiz Shaikh, “Compressive Behaviour of Sodium and Potassium Activators Synthesized Fly Ash Geopolymer at Elevated Temperatures: A Comparative Study,” *Journal of Building Engineering*, vol. 8, pp. 123-130, 2016. [[CrossRef](#)] [[Google Scholar](#)] [[Publisher Link](#)]
- [24] Wan Mastura Wan Ibrahim et al., “Chemical Distributions of Different Sodium Hydroxide Molarities on Fly Ash/Dolomite-Based Geopolymer,” *Materials*, vol. 15, no. 17, pp. 1-15, 2022. [[CrossRef](#)] [[Google Scholar](#)] [[Publisher Link](#)]
- [25] Xi Jiang et al., “A Comparative Study on Geopolymers Synthesized by Different Classes of Fly Ash after Exposure to Elevated Temperatures,” *Journal of Cleaner Production*, vol. 270, 2020. [[CrossRef](#)] [[Google Scholar](#)] [[Publisher Link](#)]
- [26] Joseph Davidovits, *Geopolymer Chemistry and Applications*, 5th ed., Geopolymer Institute, 2020. [[Publisher Link](#)]
- [27] Ahmad Azrem Azmi et al., “A Review on Fly Ash Based Geopolymer Rubberized Concrete,” *Key Engineering Materials*, vol. 700, pp. 183-196, 2016. [[CrossRef](#)] [[Google Scholar](#)] [[Publisher Link](#)]
- [28] Mir Firasath Ali, and M.M. Vijayalakshmi Natrajan, “A Review of Geopolymer Composite Thermal Properties,” *IOP Conference Series: Earth and Environmental Science, International Conference on Contemporary and Sustainable Infrastructure*, Bangalore, India, vol. 822, pp. 1-10, 2021. [[CrossRef](#)] [[Google Scholar](#)] [[Publisher Link](#)]
- [29] Hemn Unis Ahmed, Azad A. Mohammed, and Ahmed S. Mohammed, “The Role of Nanomaterials in Geopolymer Concrete Composites: A State-of-the-Art Review,” *Journal of Building Engineering*, vol. 49, 2022. [[CrossRef](#)] [[Google Scholar](#)] [[Publisher Link](#)]

- [30] Faris Matakah, Ayman Ababneh, and Ruba Aqel, "Effects of Nanomaterials on Mechanical Properties, Durability Characteristics and Microstructural Features of Alkali-Activated Binders: A Comprehensive Review," *Construction and Building Materials*, vol. 336, 2022. [[CrossRef](#)] [[Google Scholar](#)] [[Publisher Link](#)]
- [31] David W. Law et al., "Long Term Durability Properties of Class F Fly Ash Geopolymer Concrete," *Material and Structures*, vol. 48, pp. 721-731, 2014. [[CrossRef](#)] [[Google Scholar](#)] [[Publisher Link](#)]
- [32] Partha Sarathi Deb, Prabir Kumar Sarker, and Salim Barbhuiya, "Effects of Nano-Silica on the Strength Development of Geopolymer Cured at Room Temperature," *Construction and Building Materials*, vol. 101, no. 1, pp. 675-683, 2015. [[CrossRef](#)] [[Google Scholar](#)] [[Publisher Link](#)]
- [33] Pawel Sikora, Mohamed Abd Elrahman, and Dietmar Stephan, "The Influence of Nanomaterials on the Thermal Resistance of Cement-Based Composites-A Review," *Nanomaterials*, vol. 8, no. 7, pp. 1-33, 2018. [[CrossRef](#)] [[Google Scholar](#)] [[Publisher Link](#)]
- [34] Morteza Bastami, Mazyar Baghbadrani, and Farhad Aslani, "Performance of Nano-Silica Modified High Strength Concrete at Elevated Temperatures," *Construction and Building Materials*, vol. 68, pp. 402-408, 2014. [[CrossRef](#)] [[Google Scholar](#)] [[Publisher Link](#)]
- [35] Wang Yonggui et al., "Mechanical Properties and Microstructure of Basalt Fibre and Nano-Silica Reinforced Recycled Concrete after Exposure to Elevated Temperatures," *Construction and Building Materials*, vol. 247, 2020. [[CrossRef](#)] [[Google Scholar](#)] [[Publisher Link](#)]
- [36] Faiz Shaikh, and Sharany Haque, "Effect of Nano Silica and Fine Silica Sand on Compressive Strength of Sodium and Potassium Activators Synthesised Fly Ash Geopolymer at Elevated Temperatures," *Fire and Materials*, vol. 42, no. 3, pp. 324-335, 2018. [[CrossRef](#)] [[Google Scholar](#)] [[Publisher Link](#)]
- [37] Partha Sarathi Deb, Prabir Kumar Sarker, and Salim Barbhuiya, "Sorptivity and Acid Resistance of Ambient-Cured Geopolymer Mortars Containing Nano-Silica," *Cement and Concrete Composites*, vol. 72, pp. 235-245, 2016. [[CrossRef](#)] [[Google Scholar](#)] [[Publisher Link](#)]
- [38] Achile Nana et al., "Mechanical Strength and Microstructure of Metakaolin/Volcanic Ash-Based Geopolymer Composites Reinforced with Reactive Silica from Rice Husk Ash," *Materialia*, vol. 16, 2021. [[CrossRef](#)] [[Google Scholar](#)] [[Publisher Link](#)]
- [39] Jinyun Xu et al., "Research and Application Progress of Geopolymers in Adsorption: A Review," *Nanomaterials*, vol. 12, no. 17, pp. 1-23, 2022. [[CrossRef](#)] [[Google Scholar](#)] [[Publisher Link](#)]
- [40] Wyom Paul Zakka, Nor Hasanah Abdul Shukor Lim, and Ma Chau Khun, "A Scientometric Review of Geopolymer Concrete," *Journal of Cleaner Production*, vol. 280, 2021. [[CrossRef](#)] [[Google Scholar](#)] [[Publisher Link](#)]
- [41] B. Singh et al., "Geopolymer Concrete: A Review of Some Recent Developments," *Construction and Building Materials*, vol. 85, pp. 78-90, 2015. [[CrossRef](#)] [[Google Scholar](#)] [[Publisher Link](#)]
- [42] Andrés Játiva, Evelyn Ruales, and Miren Etxeberria, "Volcanic Ash as a Sustainable Binder Material: An Extensive Review," *Materials*, vol. 14, no. 5, pp. 1-32, 2021. [[CrossRef](#)] [[Google Scholar](#)] [[Publisher Link](#)]
- [43] Dali Bondar et al., "Effect of Type, form, and Dosage of Activators on Strength of Alkali-Activated Natural Pozzolans," *Cement and Concrete Composites*, vol. 33, no. 2, pp. 251-260, 2011. [[CrossRef](#)] [[Google Scholar](#)] [[Publisher Link](#)]
- [44] Sharayu Shamarao Satpute, M.N. Shirsath, and Sandeep L. Hake, "Investigation of Alkaline Activators for Fly-Ash Based Geo- Polymer Concrete," *International Journal of Advance Research and Innovative Ideas in Education*, vol. 2, no. 5, pp. 2395-4396, 2016. [[Google Scholar](#)] [[Publisher Link](#)]
- [45] R.H. Abdul Rahim et al., "Comparison of Using NaOH and KOH Activated Fly Ash-Based Geopolymer on the Mechanical Properties," *Materials Science Forum*, vol. 803, pp. 179-184, 2015. [[CrossRef](#)] [[Google Scholar](#)] [[Publisher Link](#)]
- [46] Juhuyuk Moon et al., "Characterization of Natural Pozzolan-Based Geopolymeric Binders," *Cement and Concrete Composites*, vol. 53, pp. 97-104, 2014. [[CrossRef](#)] [[Google Scholar](#)] [[Publisher Link](#)]
- [47] Thais da Silva Rocha et al., "Metakaolin-Based Geopolymer Mortars with Different Alkaline Activators (Na⁺ and K⁺)," *Construction and Building Materials*, vol. 178, pp. 453-461, 2018. [[CrossRef](#)] [[Google Scholar](#)] [[Publisher Link](#)]
- [48] C.D. Budh, and N.R. Warhade, "Effect of Molarity on Compressive Strength of Geopolymer Mortar," *International Journal of Civil Engineering Research*, vol. 5, no. 1, pp. 83-86, 2014. [[Google Scholar](#)] [[Publisher Link](#)]
- [49] Jun Zhao et al., "Effect of Elevated Temperature on Mechanical Properties of High-Volume Fly Ash-Based Geopolymer Concrete, Mortar and Paste Cured at Room Temperature," *Polymers*, vol. 13, no. 9, pp. 1-26, 2021. [[CrossRef](#)] [[Google Scholar](#)] [[Publisher Link](#)]
- [50] William Gustavo Valencia Saavedra, and Ruby Mejía de Gutiérrez, "Performance of Geopolymer Concrete Composed of Fly Ash after Exposure to Elevated Temperatures," *Construction and Building Materials*, vol. 154, pp. 229-235, 2017. [[CrossRef](#)] [[Google Scholar](#)] [[Publisher Link](#)]
- [51] Hai Yan Zhang et al., "Thermal Behavior and Mechanical Properties of Geopolymer Mortar after Exposure to Elevated Temperatures," *Construction and Building Materials Journal*, vol. 109, pp. 17-24, 2016. [[CrossRef](#)] [[Google Scholar](#)] [[Publisher Link](#)]
- [52] Patrick N. Lemougna, Kenneth J.D. MacKenzie, and U.F. Chinje Melo, "Synthesis and Thermal Properties of Inorganic Polymers (Geopolymers) for Structural and Refractory Applications from Volcanic Ash," *Ceramics International*, vol. 37, no. 8, pp. 3011-3018, 2011. [[CrossRef](#)] [[Google Scholar](#)] [[Publisher Link](#)]

- [53] Özge Topal, Mehmet Burhan Karakoç, and Ahmet Özcan, “Effects of Elevated Temperatures on the Properties of Ground Granulated Blast Furnace Slag (GGBFS) Based Geopolymer Concretes Containing Recycled Concrete Aggregate,” *European Journal of Environmental and Civil Engineering*, vol. 26, no. 10, pp. 4847-4862, 2022. [[CrossRef](#)] [[Google Scholar](#)] [[Publisher Link](#)]
- [54] Neetu Singh et al., “Effect of Aggressive Chemical Environment on Durability of Green Geopolymer Concrete,” *International Journal of Engineering and Innovative Technology*, vol. 3, no. 4, pp. 277-284, 2013. [[Google Scholar](#)] [[Publisher Link](#)]
- [55] Shoroog Alraddadi, and Hasan Assaedi, “Characterization and Potential Applications of Different Powder Volcanic Ash,” *Journal of King Saud University- Science*, vol. 32, no. 7, pp. 2969-2975, 2020. [[CrossRef](#)] [[Google Scholar](#)] [[Publisher Link](#)]
- [56] Patrick N. Lemougna et al., “Review on the Use of Volcanic Ashes for Engineering Applications,” *Resources, Conservation & Recycling*, vol. 137, pp. 177-190, 2018. [[CrossRef](#)] [[Google Scholar](#)] [[Publisher Link](#)]
- [57] F.N. Okoye, J. Durgaprasad, and N.B. Singh, “Fly Ash/Kaolin Based Geopolymer Green Concretes and their Mechanical Properties,” *Data in Brief*, vol. 5, pp. 739-744, 2015. [[CrossRef](#)] [[Google Scholar](#)] [[Publisher Link](#)]
- [58] Rossibel Churata et al., “Study of Geopolymer Composites Based on Volcanic Ash, Fly Ash, Pozzolan, Metakaolin and Mining Tailing,” *Buildings*, vol. 12, no. 8, pp. 1-12, 2022. [[CrossRef](#)] [[Google Scholar](#)] [[Publisher Link](#)]
- [59] H.K. Tchakoute et al., “Utilization of Volcanic Ashes for the Production of Geopolymers Cured at Ambient Temperature,” *Cement and Concrete Composites*, vol. 38, pp. 75-81, 2013. [[CrossRef](#)] [[Google Scholar](#)] [[Publisher Link](#)]
- [60] ASTM 618-08, Standard Specification for Coal Fly Ash and Raw or Calcined Natural Pozzolan for Use in Concrete, American Society for Testing and Materials, 2008. [[Google Scholar](#)] [[Publisher Link](#)]
- [61] Aleksandar Nikolov, Ivan Rostovsky, and Henk Nugteren, “Geopolymer Materials Based on Natural Zeolite,” *Case Studies in Construction Materials*, vol. 6, pp. 198-205, 2017. [[CrossRef](#)] [[Google Scholar](#)] [[Publisher Link](#)]
- [62] Taewan Kim, Jae Hong Kim, and Yubin Jun, “Properties of Alkali-Activated Slag Paste Using New Colloidal Nano-Silica Mixing Method,” *Materials*, vol. 12, no. 9, pp. 1-22, 2019. [[CrossRef](#)] [[Google Scholar](#)] [[Publisher Link](#)]
- [63] R. Kumar, S. Singh, and L.P. Singh, “Studies on Enhanced Thermally Stable High Strength Concrete Incorporating Silica Nanoparticles,” *Construction and Building Materials*, vol. 153, pp. 506-513, 2017. [[CrossRef](#)] [[Google Scholar](#)] [[Publisher Link](#)]
- [64] ASTM C128, ASTM C128 Standard Test Method for Density, Relative Density (Specific Gravity), and Absorption of Fine Aggregate, ASTM: West Conshohocken, 2015. [[Google Scholar](#)] [[Publisher Link](#)]
- [65] ASTM C33/C33M-08, Standard Specification for Concrete Aggregates, American Society for Testing and Materials, pp. 1-11, 2010. [[CrossRef](#)] [[Google Scholar](#)] [[Publisher Link](#)]
- [66] Jean Noël Yankwa Djobo et al., “Mechanical Properties and Durability of Volcanic Ash Based Geopolymer Mortars,” *Construction and Building Materials*, vol. 124, pp. 606-614, 2016. [[CrossRef](#)] [[Google Scholar](#)] [[Publisher Link](#)]
- [67] Fatih Kantarcı, İbrahim Türkmen, and Enes Ekinci, “Optimization of Production Parameters of Geopolymer Mortar and Concrete: A Comprehensive Experimental Study,” *Construction and Building Materials*, vol. 228, 2019. [[CrossRef](#)] [[Google Scholar](#)] [[Publisher Link](#)]
- [68] Hasan Assaedi et al., “Effect of Nanosilica on Mechanical Properties and Microstructure of PVA Fiber-Reinforced Geopolymer Composite (PVA-FRGC),” *Materials*, vol. 12, no. 21, pp. 1-11, 2019. [[CrossRef](#)] [[Google Scholar](#)] [[Publisher Link](#)]
- [69] ASTM C1437-20, Standard Test Method for Flow of Hydraulic Cement Mortar, American Society for Testing and Materials, pp. 1-2, 2020. [[CrossRef](#)] [[Google Scholar](#)] [[Publisher Link](#)]
- [70] Muhammad Talha Junaid, Amar Khennane, and Obada Kayali, “Investigation into the Effect of the Duration of Exposure on the Behaviour of GPC at Elevated Temperatures,” *MATEC Web of Conferences*, vol. 11, pp. 1-5, 2014. [[CrossRef](#)] [[Google Scholar](#)] [[Publisher Link](#)]
- [71] Rui He, Nan Dai, and Zhenjun Wang, “Thermal and Mechanical Properties of Geopolymers Exposed to High Temperature: A Literature Review,” *Advances in Civil Engineering*, vol. 2020, pp. 1-17, 2020. [[CrossRef](#)] [[Google Scholar](#)] [[Publisher Link](#)]
- [72] ASTM C109/C109M-08, Standard Test Method for Compressive Strength of Hydraulic Cement Mortars (Using 2-in. or [50-mm] Cube Specimens), American Society for Testing and Materials, pp. 1-9, 2011. [[CrossRef](#)] [[Google Scholar](#)] [[Publisher Link](#)]
- [73] Nima Farzadnia et al., “The Effect of Nano Silica on Short-Term Drying Shrinkage of POFA Cement Mortars,” *Construction and Building Materials*, vol. 95, pp. 636-646, 2015. [[CrossRef](#)] [[Google Scholar](#)] [[Publisher Link](#)]
- [74] X. Gao, Q.L. Yu, and H.J.H. Brouwers, “Characterization of Alkali Activated Slag-Fly Ash Blends Containing Nano-Silica,” *Construction and Building Materials*, vol. 98, pp. 397-406, 2015. [[CrossRef](#)] [[Google Scholar](#)] [[Publisher Link](#)]
- [75] Ali Akbar Ramezaniapour, and Mohammad Amin Moeini, “Mechanical and Durability Properties of Alkali Activated Slag Coating Mortars Containing Nanosilica and Silica Fume,” *Construction and Building Materials*, vol. 163, pp. 611-621, 2018. [[CrossRef](#)] [[Google Scholar](#)] [[Publisher Link](#)]
- [76] Elzbieta Horszczaruk et al., “The Effect of Elevated Temperature on the Properties of Cement Mortars Containing Nanosilica and Heavyweight Aggregates,” *Construction and Building Materials*, vol. 137, pp. 420-431, 2017. [[CrossRef](#)] [[Google Scholar](#)] [[Publisher Link](#)]
- [77] M.R. Karim et al., “Development of a Zero-Cement Binder Using Slag, Fly Ash, and Rice Husk Ash with Chemical Activator,” *Advances in Materials Science and Engineering*, vol. 2015, pp. 1-15, 2015. [[CrossRef](#)] [[Google Scholar](#)] [[Publisher Link](#)]

- [78] Mohsen Jafari Nadoushan, and Ali Akbar Ramezaniapour, “The Effect of Type and Concentration of Activators on Flowability and Compressive Strength of Natural Pozzolan and Slag-Based Geopolymers,” *Construction and Building Materials*, vol. 111, pp. 337-347, 2016. [[CrossRef](#)] [[Google Scholar](#)] [[Publisher Link](#)]
- [79] Hemn Unis Ahmed et al., “Compressive Strength of Geopolymer Concrete Modified with Nano-Silica: Experimental and Modeling Investigations,” *Case Studies in Construction Materials*, vol. 16, pp. 1-29, 2022. [[CrossRef](#)] [[Google Scholar](#)] [[Publisher Link](#)]
- [80] Ilknur Bekem Kara, “The Effect of Nano Silica on the Properties of Cement Mortars Containing Micro Silica at Elevated Temperatures,” *Romanian Journal of Materials*, vol. 49, no. 4, pp. 518-526, 2019. [[Google Scholar](#)] [[Publisher Link](#)]
- [81] M. Komljenović, Z. Baščarević, and V. Bradić, “Mechanical and Microstructural Properties of Alkali-Activated Fly Ash Geopolymers,” *Journal of Hazardous Materials*, vol. 181, no. 1-3, pp. 35-42, 2010. [[CrossRef](#)] [[Google Scholar](#)] [[Publisher Link](#)]
- [82] D.J. Ilham et al., “Utilization of Volcanic Ashes for Geopolymer Based on Alkaline Activator and Solid-Liquid Ratio,” *IOP Conference Series: Earth and Environmental Science*, 2nd International Conference on Disaster and Management, Indonesia, vol. 708, no. 1, pp. 1-6, 2021. [[CrossRef](#)] [[Google Scholar](#)] [[Publisher Link](#)]
- [83] Zihui Peng, “Microstructural and ²⁹Si MAS NMR Spectroscopic Evaluations of Alkali Cationic Effects on Fly Ash Activation,” *Cement and Concrete Composites*, vol. 57, pp. 34-43, 2015. [[CrossRef](#)] [[Google Scholar](#)] [[Publisher Link](#)]
- [84] Seick Omar Sore et al., “Comparative Study on Geopolymer Binders Based on Two Alkaline Solutions (NaOH and KOH),” *Journal of Minerals and Materials Characterization and Engineering*, vol. 8, no. 6, pp. 407-420, 2020. [[CrossRef](#)] [[Google Scholar](#)] [[Publisher Link](#)]
- [85] F.N. Okoye, J. Durgaprasad, and N.B. Singh, “Mechanical Properties of Alkali Activated Flyash/Kaolin Based Geopolymer Concrete,” *Construction and Building Materials*, vol. 98, pp. 685-691, 2015. [[CrossRef](#)] [[Google Scholar](#)] [[Publisher Link](#)]
- [86] Lais Alves, Nordine Leklou, and Silvio De Barros, “A Comparative Study on the Effect of different Activating Solutions and Formulations on the Early Stage Geopolymerization Process,” *Matec Web of Conferences*, vol. 322, pp. 1-13, 2020. [[CrossRef](#)] [[Google Scholar](#)] [[Publisher Link](#)]
- [87] Y. Luna-Galiano et al., “Properties of Fly Ash and Metakaolin Based Geopolymer Panels under Fire Resistance Tests,” *Construction Materials*, vol. 65, no. 319, pp. 1-13, 2015. [[CrossRef](#)] [[Google Scholar](#)] [[Publisher Link](#)]
- [88] İbrahim Türkmen et al., “Fire Resistance of Geopolymer Concrete Produced from Elazığ Ferrochrome Slag,” *Fire and Materials*, vol. 40, no. 6, pp. 836-847, 2016. [[CrossRef](#)] [[Google Scholar](#)] [[Publisher Link](#)]
- [89] F.U.A. Shaikh, and V. Vimonsatit, “Compressive Strength of Fly-Ash-Based Geopolymer Concrete at Elevated Temperatures,” *Fire and Materials*, vol. 39, no. 2, pp. 174-188, 2014. [[CrossRef](#)] [[Google Scholar](#)] [[Publisher Link](#)]
- [90] Mukund Lahoti et al., “Effect of Alkali Cation Type on Strength Endurance of Fly Ash Geopolymers Subject to High Temperature Exposure,” *Materials and Design*, vol. 154, pp. 8-19, 2018. [[CrossRef](#)] [[Google Scholar](#)] [[Publisher Link](#)]
- [91] Patrick N. Lemougna et al., “Influence of the Activating Solution Composition on the Stability and Thermo-Mechanical Properties of Inorganic Polymers (Geopolymers) from Volcanic Ash,” *Construction and Building Materials*, vol. 48, pp. 278-286, 2013. [[CrossRef](#)] [[Google Scholar](#)] [[Publisher Link](#)]
- [92] R. Anjusha, and S. Bindu, “Influence of Nanosilica on Properties of Ternary Blended Concrete,” *International Journal of Science & Engineering Research*, vol. 5, no. 7, pp. 575-582, 2014. [[Google Scholar](#)] [[Publisher Link](#)]
- [93] T. Bakharev, “Thermal Behaviour of Geopolymers Prepared Using Class F Fly Ash and Elevated Temperature Curing,” *Cement and Concrete Research*, vol. 36, no. 6, pp. 1134-1147, 2006. [[CrossRef](#)] [[Google Scholar](#)] [[Publisher Link](#)]
- [94] K. Zulkifly et al., “Review of Geopolymer Behaviour in Thermal Environment,” *IOP Conference Series: Materials Science and Engineering, International Conference on Innovative Research - ICIR Euroinvent*, Iasi, Romania vol. 209, pp. 1-9, 2017. [[CrossRef](#)] [[Google Scholar](#)] [[Publisher Link](#)]
- [95] K.M. Klima et al., “Enhancing the Thermal Performance of Class F Fly Ash-Based Geopolymer by Sodalite,” *Construction and Building Materials*, vol. 314, pp. 1-13, 2022. [[CrossRef](#)] [[Google Scholar](#)] [[Publisher Link](#)]
- [96] Faiz Uddin Ahmed Shaikh, Sharany Haque, and Jay Sanjayan, “Behavior of Fly Ash Geopolymer as Fire Resistant Coating for Timber,” *Journal of Sustainable Cement-Based Materials*, vol. 8, no. 5, pp. 259-274, 2019. [[CrossRef](#)] [[Google Scholar](#)] [[Publisher Link](#)]
- [97] Rafia Firdous, Dietmar Stephan, and Jean Noël Yankwa Djobo, “Natural Pozzolan Based Geopolymers: A Review on Mechanical, Microstructural and Durability Characteristics,” *Construction and Building Materials*, vol. 190, pp. 1251-1263, 2018. [[CrossRef](#)] [[Google Scholar](#)] [[Publisher Link](#)]
- [98] Ali Nazari et al., “Thermal Shock Reactions of Ordinary Portland Cement and Geopolymer Concrete: Microstructural and Mechanical Investigation,” *Construction and Building Materials*, vol. 196, pp. 492-498, 2019. [[CrossRef](#)] [[Google Scholar](#)] [[Publisher Link](#)]
- [99] Faiz Uddin Ahmed Shaikh, “Effects of Slag Content on the Residual Mechanical Properties of Ambient Air-Cured Geopolymers Exposed to Elevated Temperatures,” *Journal of Asian Ceramic Societies*, vol. 6, no. 4, pp. 342-358, 2018. [[CrossRef](#)] [[Google Scholar](#)] [[Publisher Link](#)]